NASA CR-189262 CSC/TM-76/6104

(NASA-CR-189262) COMMUNICATIONS TECHNOLOGY SATELLITE (CTS) POSTLAUNCH REPORT (Computer Sciences Corp.) 55 p

N92-70362

Unclas

Z9/18 0077071

CSC/TM-76/6104

# COMMUNICATIONS TECHNOLOGY SATELLITE (CTS)

# POSTLAUNCH REPORT

Prepared for

GODDARD SPACE FLIGHT CENTER

By

COMPUTER SCIENCES CORPORATION

Under

Contract NAS 5-11999
Task Assignment 532


Prepared by:

G K Tandon 5/4/76
G. K. Tandon Date

P. M. Smith 5/5/76
P. M. Smith Date

Approved by:

M. Joseph 5/4/76
M. Joseph Date
Section Manager

D. J. Stewart Date
Technical Area Manager

ABSTRACT

This document describes the support provided by the Goddard Space Flight Center (GSFC) Attitude Determination and Control Section and its contractor Computer Sciences Corporation during the 2 weeks immediately following the launch of the Communications Technology Satellite (CTS) on January 17, 1976. Results concerning attitude sensor performance, attitude and bias determination, and attitude control system performance are presented. Included also are brief descriptions of the spinning attitude sensors and attitude control system and their final alignment data. A detailed discussion of attitude sensors, attitude control system, and attitude determination and control procedures is given in Reference 1. The reader is assumed to be familiar with the contents of that document.

TABLE OF CONTENTS

## LIST OF ILLUSTRATIONS

Figure

## LIST OF ILLUSTRATIONS (Cont'd)



## LIST OF TABLES

## SECTION 1 - OVERVIEW

This section reviews the major events of the Communications Technology Satellite (CTS) mission which occurred during the time from lift-off to station acquisition, described from the perspective of the Attitude Determination and Control Section at Goddard Space Flight Center (GSFC).

CTS was launched from Cape Kennedy at 23 hours, 27 minutes, 54 seconds Greenwich mean time (GMT) on January 17, 1976. Injection into the transfer orbit occurred at 23 hours, 52 minutes on January 17, and a satisfactory transfer orbit was achieved with the following parameters:

| Parameter | Description |
|---|---|
| Semimajor axis | 24579.1 kilometers |
| Eccentricity | 0.733086 |
| Inclination | 27.2013 degrees |
| Right ascension of ascending mode | 288.005 degrees |
| Argument of perigee | 178.824 degrees |
| Mean anomaly | 0.439642 degrees |
| Epoch date (GMT) | January 17, 1976 |
| Epoch time | 23 hours, 52 minutes, 0 seconds |
| Spin axis right ascension | 197.52 degrees |
| Spin axis declination | -22.53 degrees |

The perigee height was 2.38 kilometers below the nominal value but was within the expected dispersion and was therefore not corrected. A chronology of the main attitude support events from lift-off to station acquisition is as follows:

| Event | Date (YY:MM:DD) | Time (GMT) (HH:MM) |
|---|---|---|
| Switch to Sun sensor-W | 76/01/18 | 02:20 |
| Switch back to Sun sensor-E | 76/01/18 | 02:27 |

| Event | Date (YY:MM:DD) | Time (GMT) (HH:MM) |
|---|---|---|
| First attempt to reorient to apogee motor firing attitude (AMFA)[1] | 76/01/18 | 15:11 |
| Reorientation from injection attitude (INJA) to system verification attitude (SVA) | 76/01/19 | 03:28 |
| Reorientation from SVA to AMFA | 76/01/19 | 23:08 |
| Trim for AMFA | 76/01/20 | 08:45 |
| Apogee motor firing | 76/01/20 | 20:41 |
| Reorientation from AMFA to drift orbit normal attitude (DONA) | 76/01/20 | 22:40 |

During the interval from January 20 to January 29, attitude was determined on a daily basis in support of station acquisition orbit maneuvers. On January 30 and 31, the despin maneuver from 60 revolutions per minute (rpm) to 1.5 rpm was monitored through the attitude support system at GSFC.

[1]At this time when latch valve 1 (LV1 in Figure 2-1) was opened, pressure of the west tank fell to zero. Further attempts at reorientation were postponed until the problem was resolved.

# SECTION 2 - ATTITUDE SENSORS AND CONTROL SYSTEM

## 2.1 ATTITUDE SENSORS

The CTS is configured with the following attitude sensors:

- Two spinning Sun sensors (SSS-E, SSS-W)
- Two spinning Earth sensors (SES-E, SES-W)
- Five nonspinning Sun sensors
- Two nonspinning Earth sensors

The four "spinning" sensors were used for attitude determination during the phases of the mission supported by the attitude support system at GSFC, i.e., during the transfer and drift orbits in which the spacecraft was spinning at 60 rpm. The seven "nonspinning" sensors are used by the closed loop attitude control system which was activated after the spacecraft had been despun. The data from the nonspinning Sun sensors was available during the transfer and drift orbit phases and could have been used in case of failure of spinning Sun sensors. A detailed description of the attitude sensors and onboard processing and telemetering of spinning sensor data is given in Reference 1.

### 2.1.1 Final Alignment Data of the Spinning Attitude Sensors

The numerical data on the spinning attitude sensors and telemetry system is given in Reference 1. The final prelaunch measured alignment values of the spinning attitude sensor's azimuth and elevation are as follows:

| Parameter | Value (degrees) |
|---|---|
| Azimuth angle of spinning Sun and Earth sensor line of sight from spacecraft geometric x-axis: | |
| SSS-E | 0.234 |
| SSS-W | 180.204 |
| SES-E | 0.246 |
| SES-W | 180.148 |

| Parameter | Value (degrees) |
|---|---|
| Angle of spinning Sun and Earth sensor line of sight from spacecraft spin axis: | |
| SSS-E | 89.966 |
| SSS-W | 89.929 |
| SES-E | 84.964 |
| SES-W | 95.002 |

### 2.1.2 SES Leading Edge Output Anomaly

During the spacecraft prelaunch tests, it was found that the SES-W produced a leading edge output even when the Earth stimulus was absent (Reference 2). Detailed testing analysis indicated that when the sensor is scanning the Earth, both leading and trailing edge pulses will occur, resulting in stable time intervals. When the sensor is scanning only space, the trailing edge Earth interval will be zero, and the leading edge Earth interval will be either zero or approximately equal to the Sun pulse interval, depending on the bias state in the leading edge thresholding circuitry. This anomalous behavior was observed only for the SES-W during tests. However, after launch both Earth sensors were observed to give spurious leading edge output when they were not scanning the Earth. These spurious data were rejected by manually editing the raw telemetry data. When the Earth sensors were scanning the Earth, they performed nominally.

### 2.1.3 Encoder Clock Rate Variations

During the spacecraft prelaunch tests, it was found that the encoder clock rate varies with temperature from nominal (15,360 hertz) to 70 hertz low, i.e., to 14,270 hertz (References 3 and 4). The temperature of the spacecraft in spinning phase was expected to be near the middle of the range (25 degrees Centigrade to 30 degrees Centigrade). Therefore, it was recommended that initially a clock rate of 15,325 hertz be used. For greater accuracy during the mission, the encoder clock rate was measured at Spaceflight Tracking and Data Network

(STDN) stations at intervals and manually changed in the attitude support system. The encoder clock rate during the spin-stabilized period of the mission varied between 15,330 hertz and 15,303 hertz. The only significant effect due to error in the encoder clock rate will be in the observed spin rate of the spacecraft. The error in the computed rotation angles will be generally negligible because in the computation of rotation angle from crossing interval, in the main term, the encoder clock rate occurs in both the numerator and the denominator. Only the portion of rotation angle to be attributed to fixed electronic time delay (7.7 milliseconds) is affected by errors in the encoder clock rate.

## 2.2 ATTITUDE CONTROL SYSTEM

A schematic diagram of the spacecraft's reaction control system (RCS) is shown in Figure 2-1. The RCS contains two "high-thrust" engines (HTEs) which were used for attitude and orbit maneuvers during the portions of the mission supported by GSFC. The RCS also includes 16 "low-thrust" engines (LTEs) which were employed after GSFC's control of the mission had terminated. During the portions of the mission supported by GSFC, LTEs could be used to change the spin rate of the spacecraft if the spin rate got outside the nominal 50-rpm-to-75-rpm range, and LTEs $P_2$, $P_4$, E, and W were available as backups for HTEs.

Of the two HTEs, called the axial high-thrust engine (Ax HTE) and the radial high-thrust engine (Ra HTE), only the Ax HTE was employed by the Attitude Control Support System (ACSS). For attitude reorientations the Ax HTE was fired in a pulsed mode, i.e., one pulse was generated in each spin revolution of the spacecraft. The LTEs were not used during the portions of the mission supported by GSFC. Detailed description of the RCS is given in Reference 1.

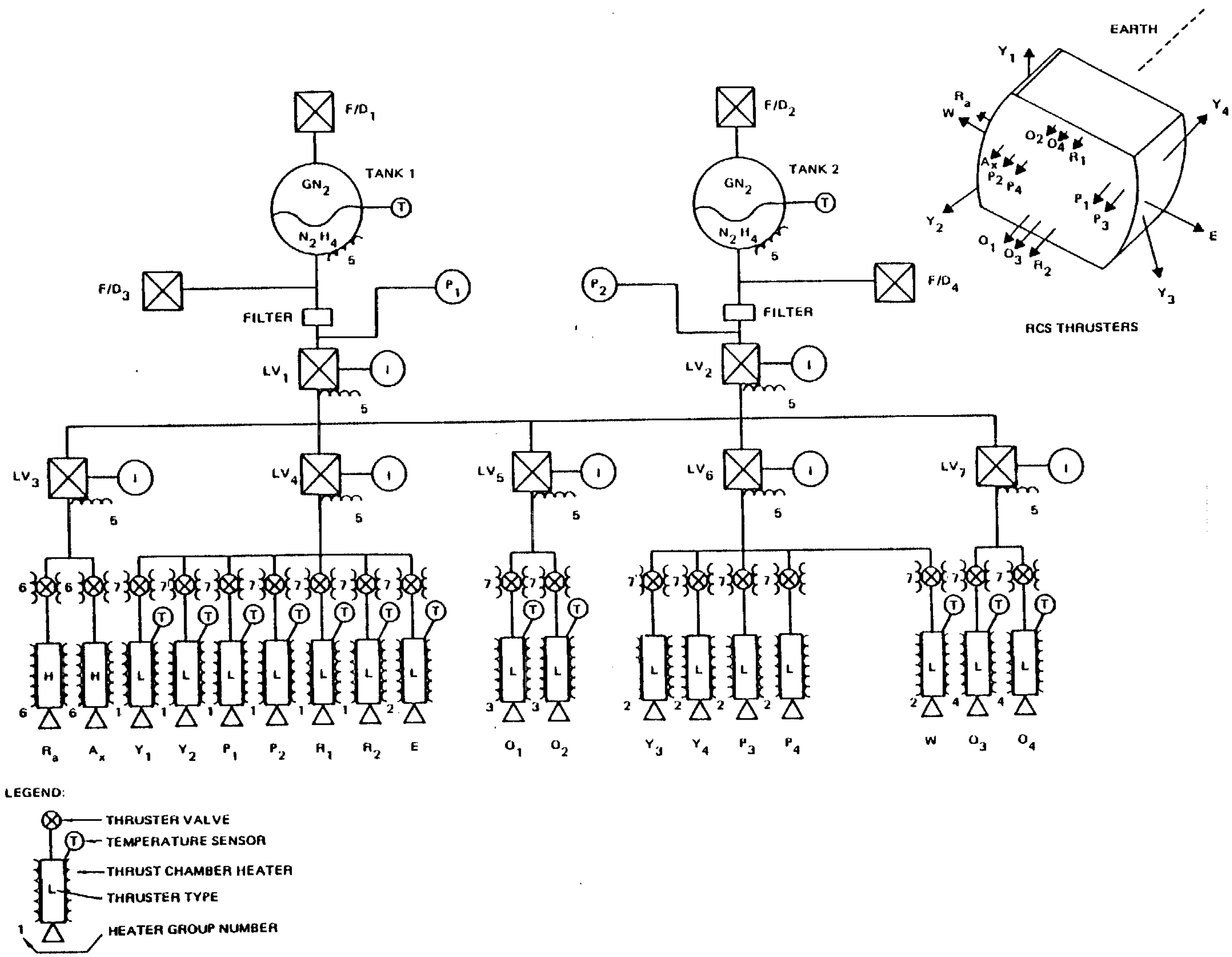


Figure 2-1. RCS Propulsion Schematic Diagram

### 2.2.1 High-Thrust Engine Performance and Support

During a pulsed mode firing of the active HTE, one pulse is generated in each spin revolution of the spacecraft.

Each pulse is initiated automatically, by the onboard electronics equipment, at a selected time delay ($t_d$) after the Sun sighting reference pulse is generated by the onboard spinning Sun sensor system. The same $t_d$ value is used for all pulses in any single train. This value is determined by the ACSS and transmitted to the spacecraft.

The nominal width of the electronic firing signal which initiates and terminates each pulse is 0.134 second. The number of pulses (n) required to be fired for a given maneuver was computed by the ACSS. Details of the engine test performance parameters are given in Reference 1.

### 2.2.2 Final Alignment Data of the High-Thrust Engines

Figure 2-2 shows the nominal locations and orientations of the thrust vectors ($\vec{F}_R$ and $\vec{F}_A$) of the radial and axial engines. The final prelaunch measured alignment values, prelaunch numerical data on the attitude control system, and basic data on the spacecraft mass properties are as follows:

| Parameter | Value |
|---|---|
| Azimuth angle of thrust vector from spacecraft geometric x-axis: | |
| Ax HTE (degrees) | 355.275 |
| Ra HTE (degrees) | 7.914 |
| P2 (degrees) | 0.000 |
| P4 (degrees) | 0.000 |
| Elevation above spin plane: | |
| Ax HTE (degrees) | + 82.652 |
| Ra HTE (degrees) | + 1.203 |
| P2 (degrees) | + 89.911 |
| P4 (degrees) | + 89.939 |
| Apogee boost motor, fuel weight (pounds) | 686.942 |

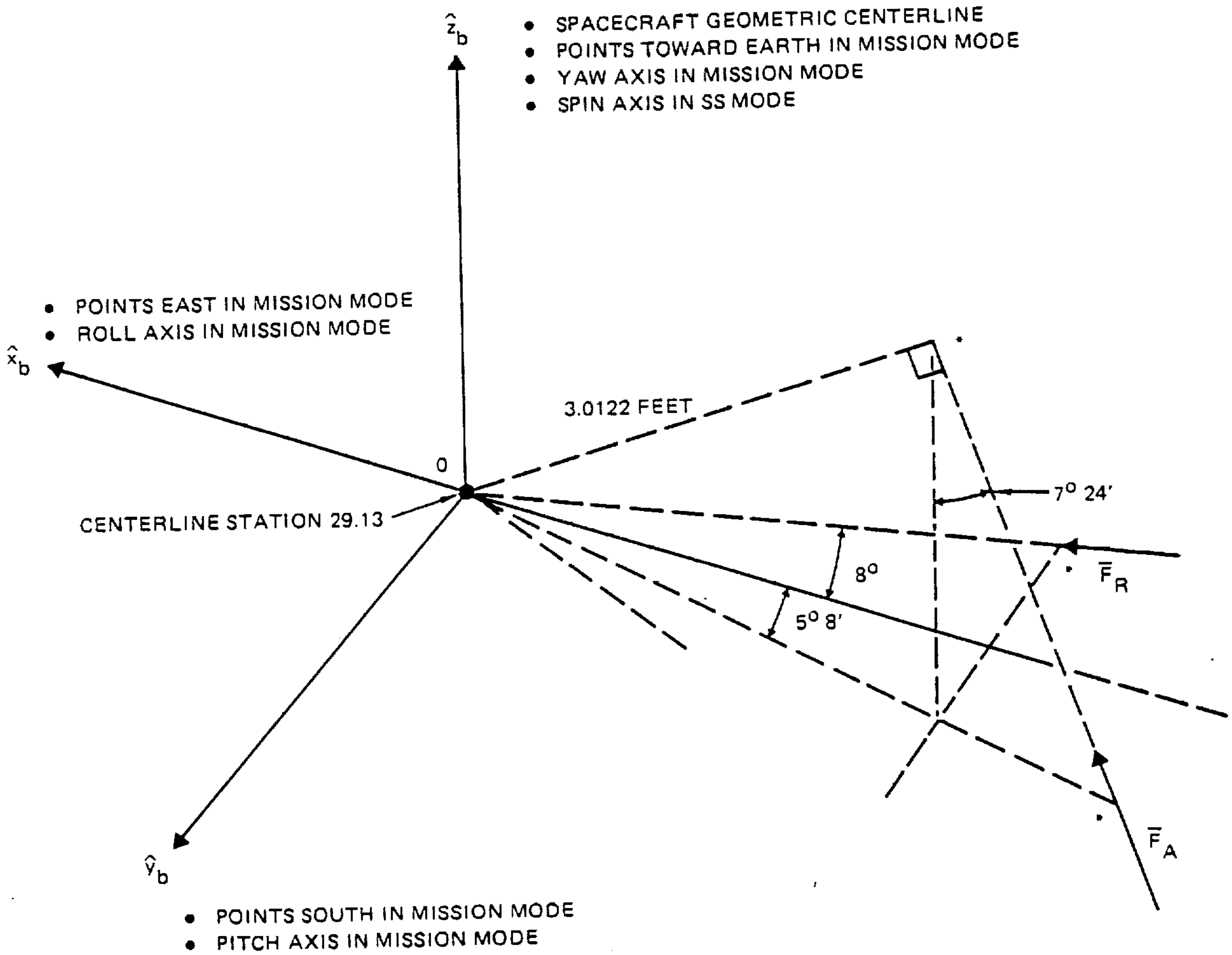


$\bar{F}_R$ – FORCE VECTOR FROM RADIAL HIGH-THRUST ENGINE

$\bar{F}_A$ – FORCE VECTOR FROM AXIAL HIGH-THRUST ENGINE

*THESE POINTS DO NOT SIGNIFY THE LOCATIONS OF THE ENGINES.

Figure 2-2. High-Thrust Engine Force Vector Nominal Locations and Directions

| Parameter | Value |
|---|---|
| RCS fuel (hydrazine) weight (pounds) | 54.737 |
| RCS fuel tank pressure at loading (pounds per square inch) | 354.50 |
| RCS fuel tank temperature at loading (degrees Fahrenheit) | 72 |
| Total spacecraft weight at lift-off (pounds) | 1490.506 |

Other prelaunch nominal numerical data is given in Reference 1.

# SECTION 3 - POSTLAUNCH ANALYSIS OF ATTITUDE SENSOR DATA

Data from both spinning Sun sensors and both spinning Earth sensors was of excellent quality. Noise from the Sun sensor data was less than the granularity of the hardware. Noise for the Earth sensor rotation angle data was typically of the order of 0.02 degree (as given by Optical Aspect Attitude and Bias Determination (OABIAS) solutions over large data spans). This noise is attributed to the granularity of the spacecraft clock (one clock pulse equals approximately 0.024 degree).

## 3.1 SPIN RATE

The spin rate of the spacecraft at constant attitudes remained constant over large intervals, indicating absence of significant nutation. Figure 3-1 shows the spin rate of the spacecraft over a period of 3 hours at injection attitude. The observed systematic increase in spin rate in Figure 3-1 is attributed to a systematic decrease in the encoder clock rate during the data span as discussed in Section 2.1.3. The decrease in encoder clock rate during the above-mentioned data span was confirmed from the measured values at STDN stations. Occasional fluctuations in spin rate between adjacent buckets (Figure 3-1) are attributed to noise and encoder clock granularity (approximately 0.024 degree at 60 rpm).

## 3.2 SUN ANGLE DATA

At all times during the mission, the prime spinning Sun sensor provided Sun angle data that was accurate to within the granularity of this sensor (0.25 degree). No flipping of this angle data between adjacent Sun buckets was observed (see Figure 3-2). For the short period of time in which the redundant Sun sensor (west) was active, the Sun angle data remained identical to that provided by the prime spinning Sun sensor. The smooth transition of the Sun angle between adjacent buckets indicated that nutation of the spacecraft was less than one-eighth of a degree.

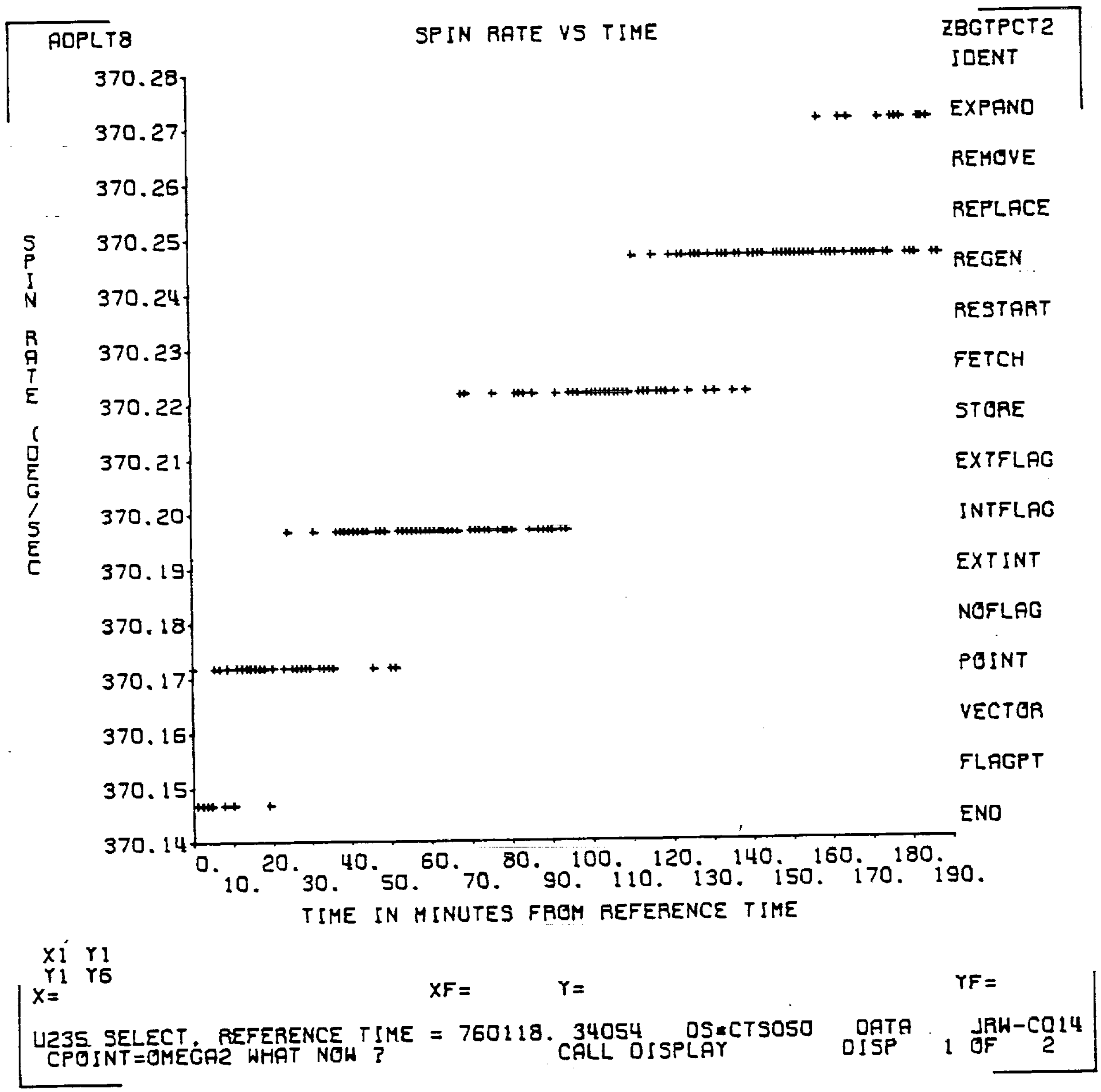


Figure 3-1. Spin Rate Versus Time Plot

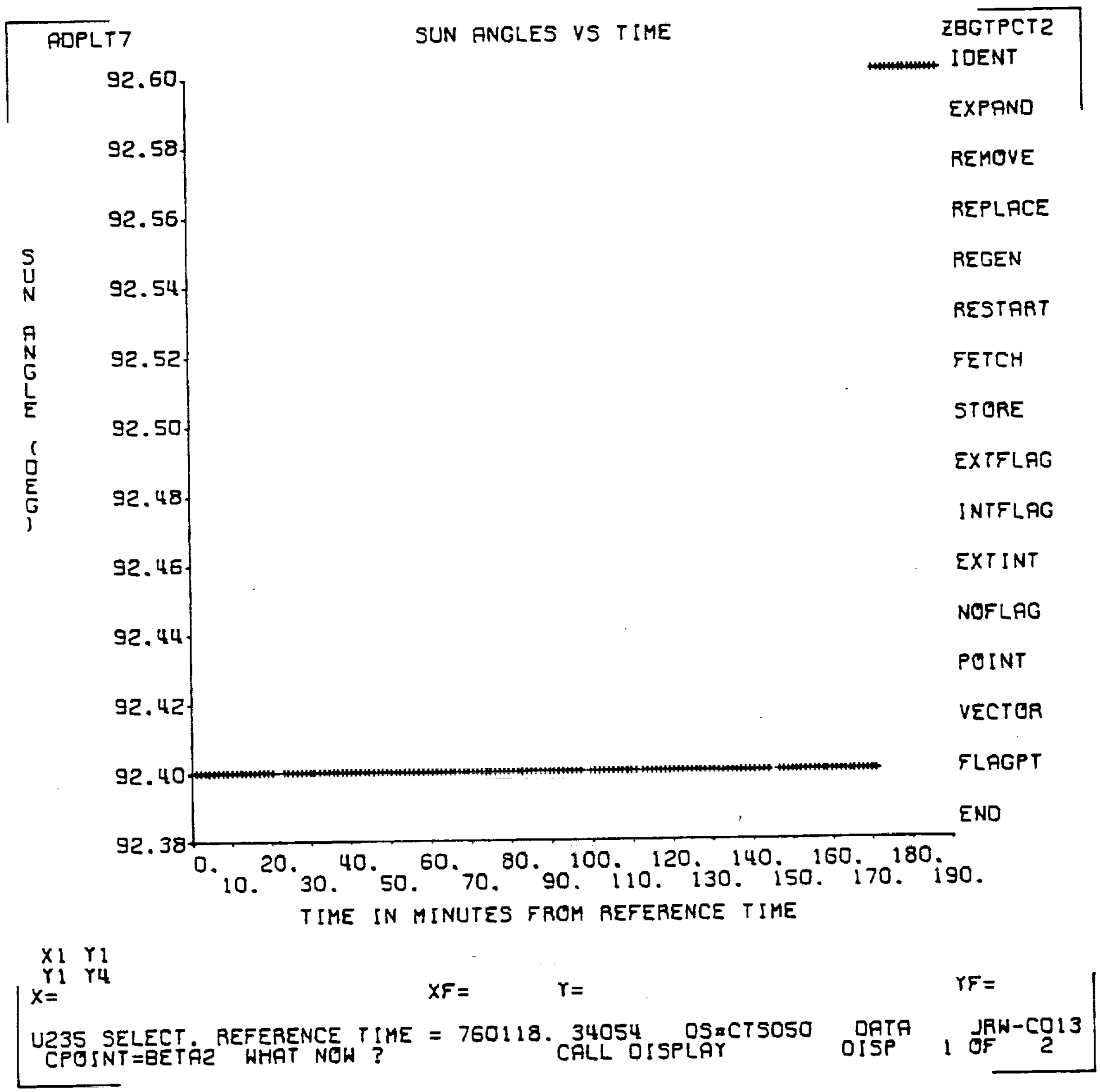


Figure 3-2. Sun Angle Versus Time Plot

## 3.3 ROTATION ANGLE DATA FROM SPINNING EARTH SENSORS

Although the specification for the units states that they shall meet their specified accuracies for attitudes between 10,000 and 20,000 nautical miles, both spinning Earth sensors performed adequately throughout all Earth coverage regions for the transfer orbit. An anomaly shown by both east and west Earth sensors was the random ficticious indication of a sky-to-Earth boundary crossing when no Earth coverage was available. This erroneous data was rejected by manually editing the raw telemetry data arrays. Figure 3-3 shows this effect occurring for the west Earth sensor. Figures 3-3 and 3-4 show rotation angle data at first apogee in the transfer orbit, and Figures 3-5 and 3-6 show similar data in the drift orbit.

### 3.3.1 Pagoda Effect

This anomaly (Reference 1) affects the behavior of attitude data at small Earth widths and is due to the electronic response of the infrared bolometer and its associated electronics. Rotation angle data for apogee 1 (Figures 3-7 and 3-8) clearly demonstrates that this distortion is present. In these figures solid lines represent predicted rotation angles as calculated from the determined attitude, and the symbol "+" represents the observed rotation angle. Using the analytical results for CTS and previous satellite data (Reference 1), all rotation angle data for Earth widths of less than 12 degrees were arbitrarily rejected. Data for Earth widths larger than 12 degrees was considered to be unaffected by this distortion and could be reliably used for attitude determination.

### 3.3.2 Perigee Data

Perigee data (perigees 6 and 7) for the transfer orbit played an important role in attitude determination. The wide range of geometrical conditions present for perigee data make the data very sensitive to the fitting parameters. Consequently the combination of perigee data with an equal section of apogee data enabled a more accurate attitude determination result to be obtained. Perigee

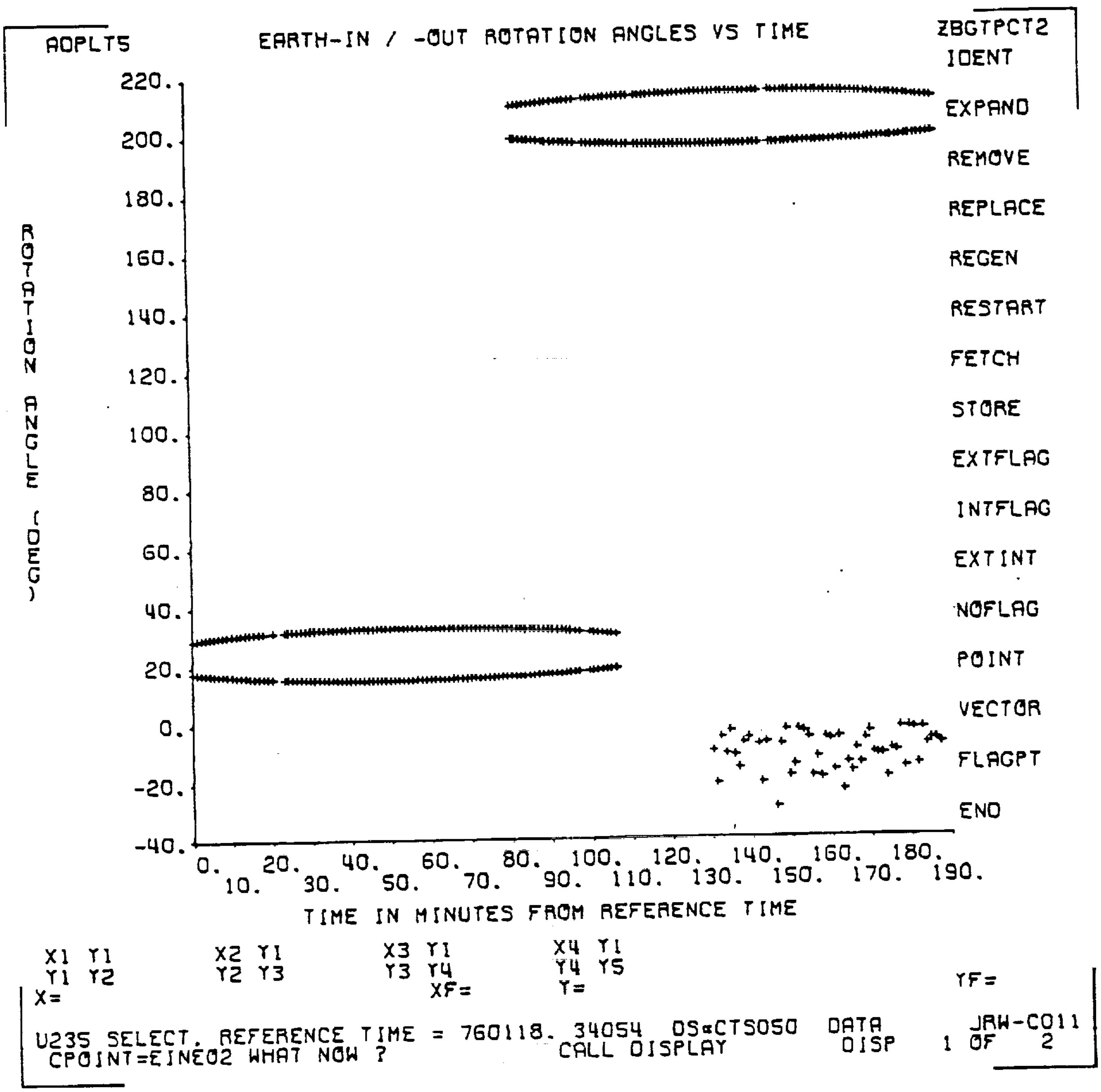


Figure 3-3. Earth-In/Earth-Out Rotation Angles Versus Time at First Apogee in Transfer Orbit

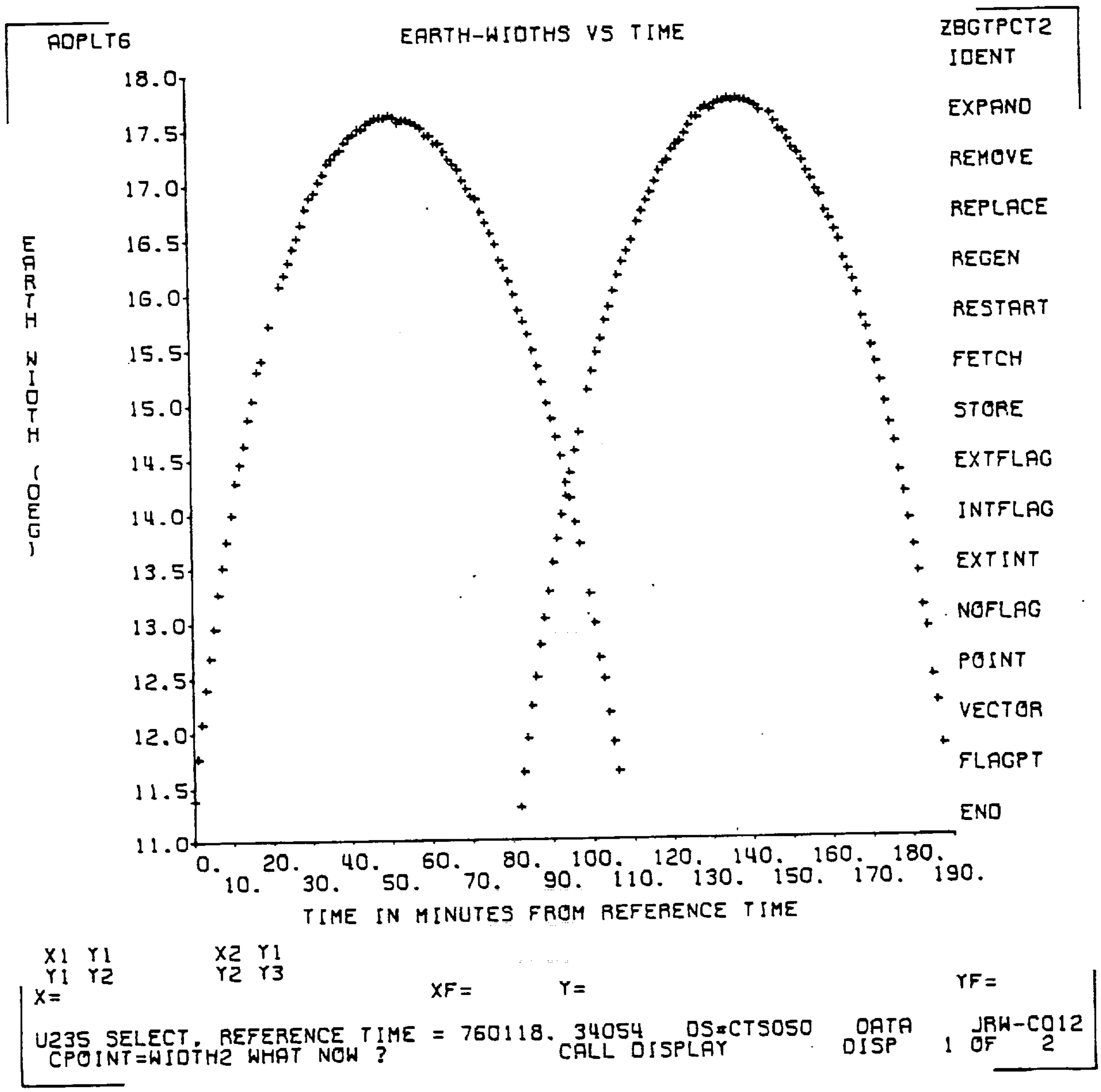


Figure 3-4. Earth Width Versus Time at First Apogee in Transfer Orbit

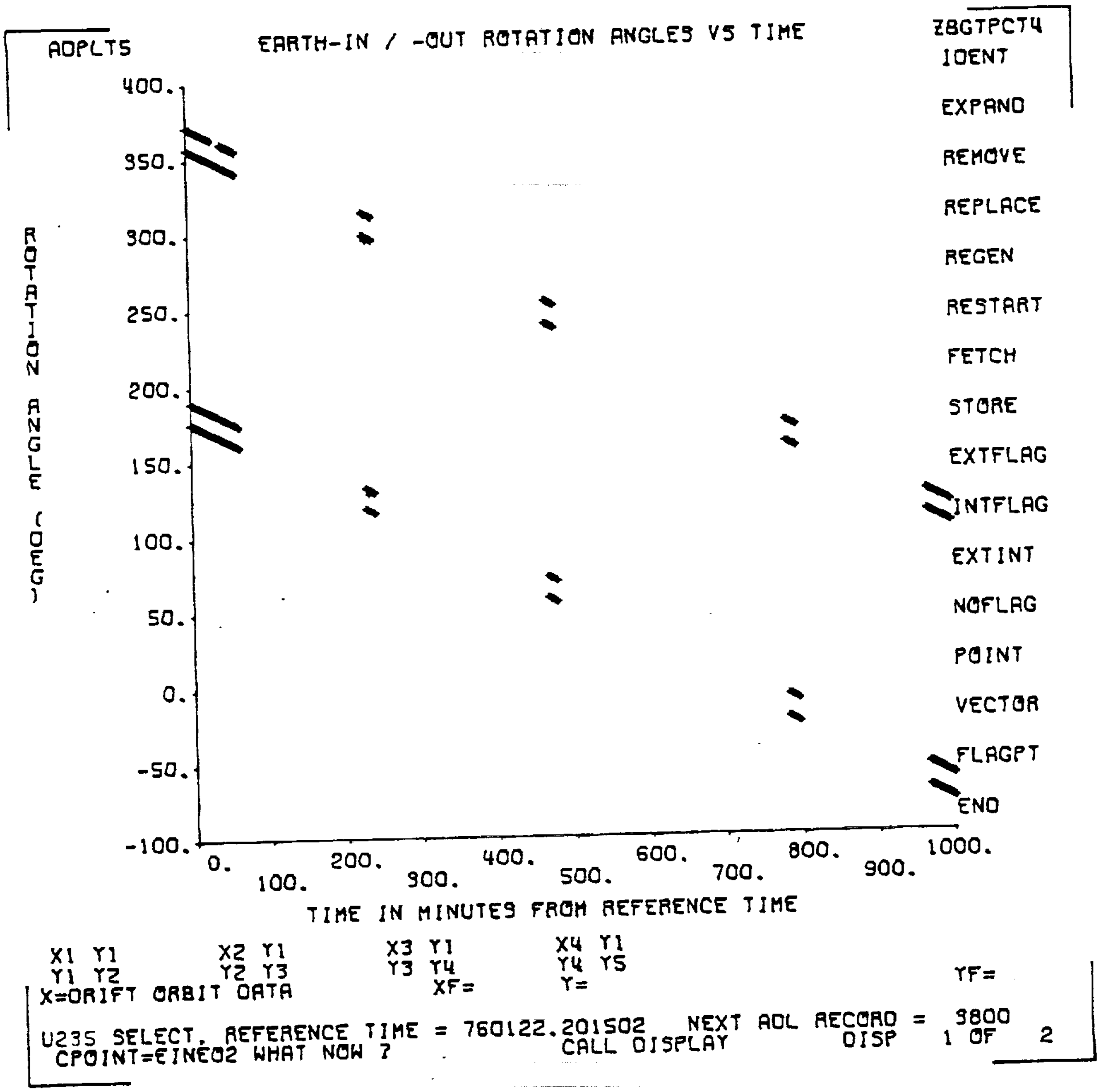


Figure 3-5. Earth-In/Earth-Out Rotation Angles Versus Time in Drift Orbit

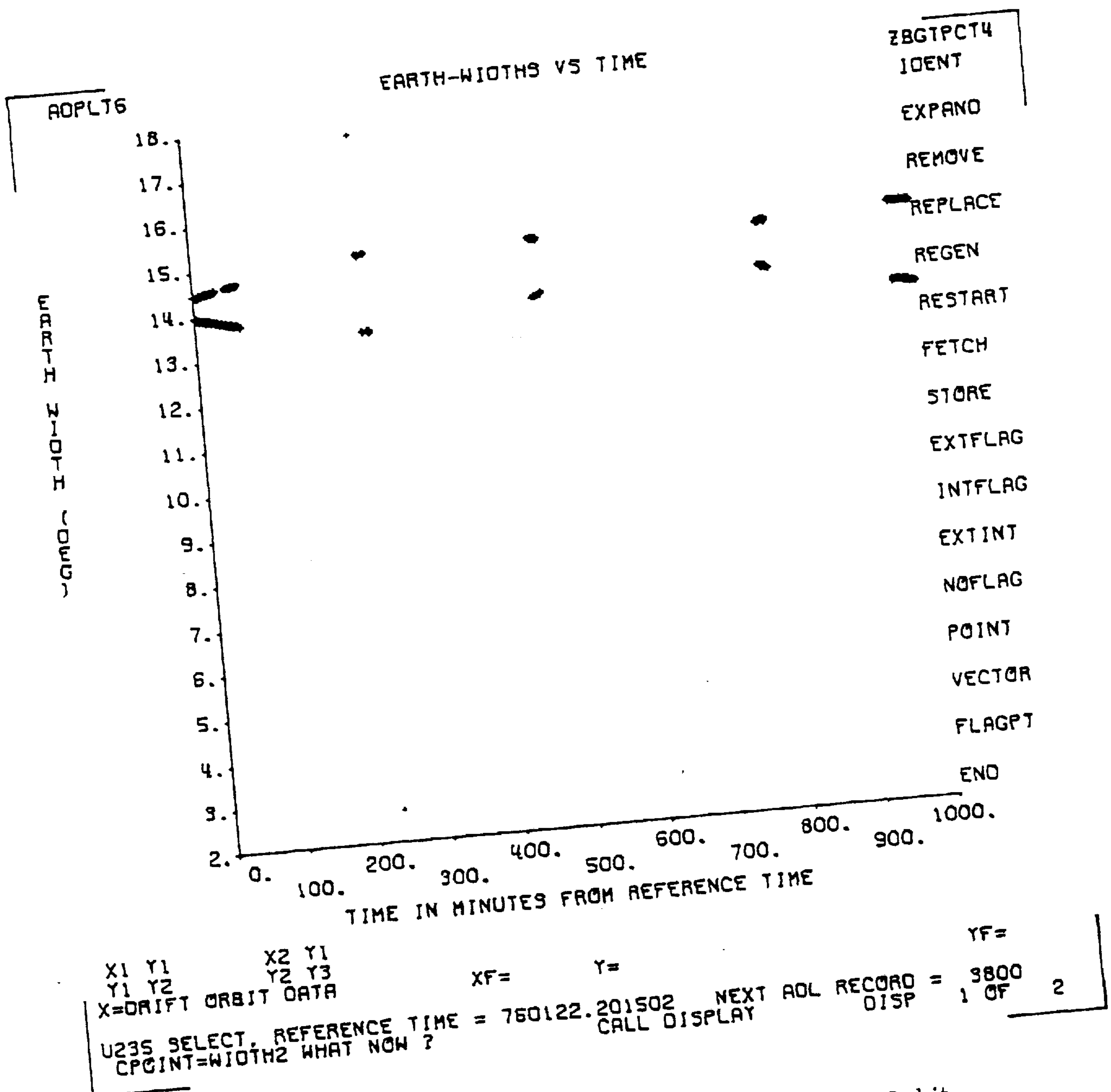


Figure 3-6. Earth Widths Versus Time in Drift Orbit

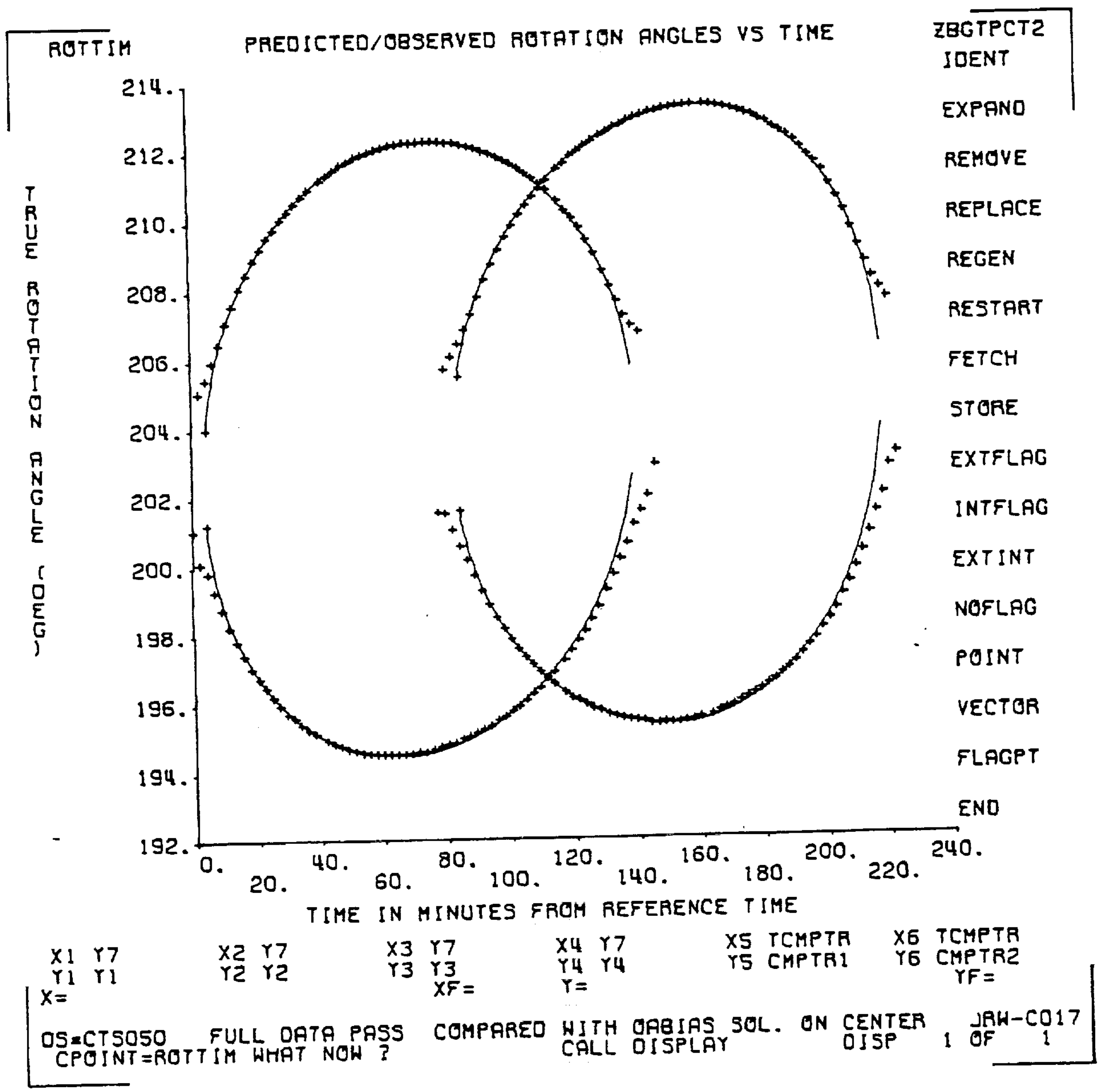


Figure 3-7. Predicted/Observed Rotation Angles Versus Time at First Apogee (Full Data Pass for Both Earth Sensors)

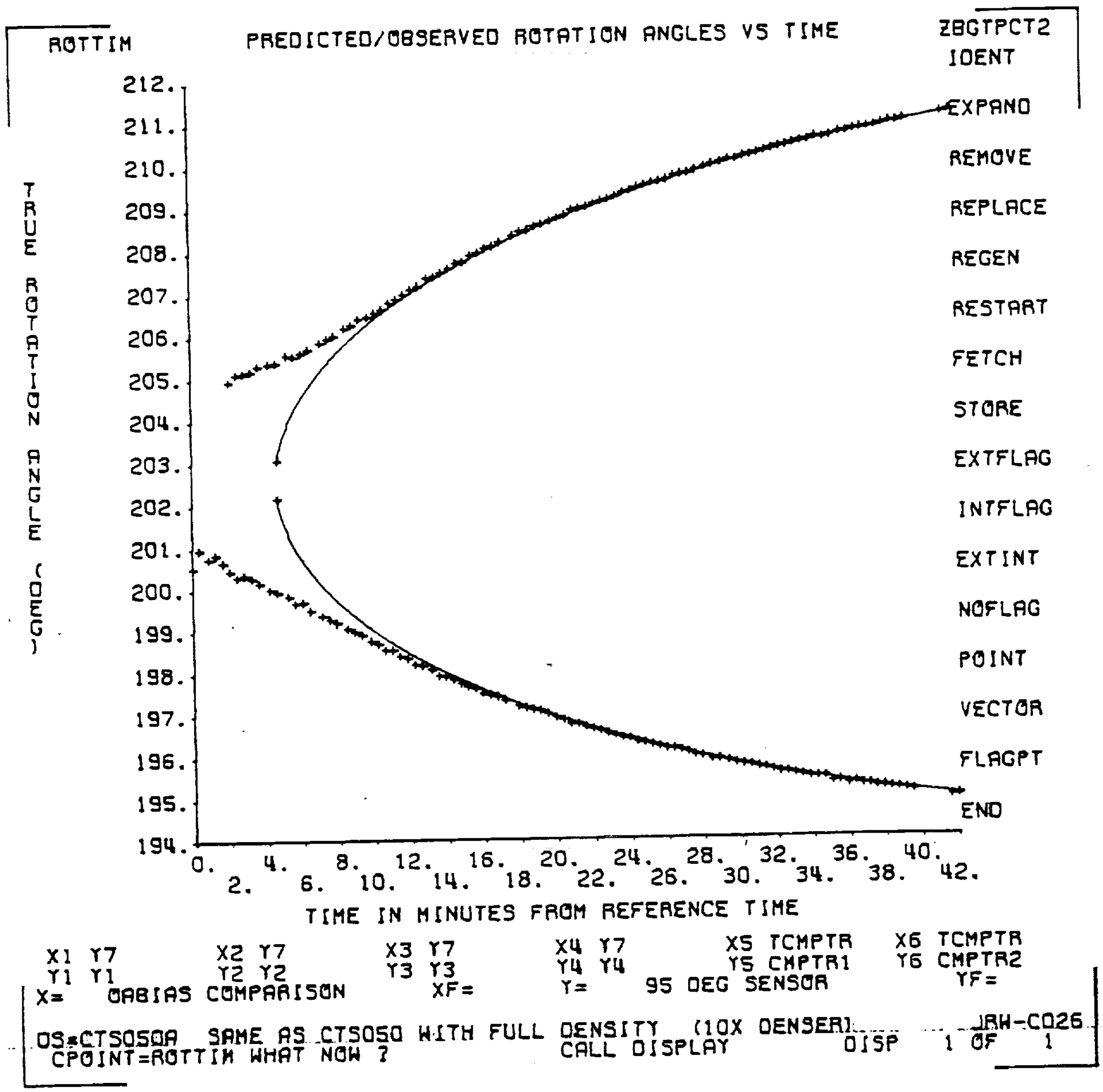


Figure 3-8. Predicted/Observed Rotation Angles Versus Time for SES-W at First Apogee (All Points Shown) (Solid Line is Predicted Plot From Computed Attitude)

data prior to perigee 6 was present in too small a quantity to allow effective use to be made of it.

## 3.4 SENSOR BIASES

### 3.4.1 Bias Determination

In determining the sensor biases for the CTS mission, prelaunch analysis (Reference 1) had indicated the following conclusions:

- Injection attitude provides poor geometry data for accurate bias determination to be possible.
- Apogee motor firing (AMF) is the principal attitude for bias determination activities prior to AMF.
- For AMF attitude the major problem for bias determination is the high correlation of sensor mounting angle and Sun angle (caused by the Sun vector, nadir vector, and attitude being nearly coplanar).
- For AMF attitude in the drift orbit, a second Earth ellipse exists, providing a greater variation in the available geometry and, therefore, improving the potential for bias determination.
- The best geometry for bias determination on CTS occurs 20 degrees from orbit normal, because it is here that the largest variation in the geometrical data is present.
- For the spacecraft at orbit normal, a full program of bias determination is no longer possible due to the redundancy of the data.

The general procedure for determining biases for the CTS sensors involved using prelaunch analysis findings as guidelines; thus, in order to eliminate the pagoda effect, only data for Earth widths greater than 12 degrees was used in solving for the biases. For AMF attitude, because of the correlation between sensor mounting angle and Sun angle, one of these parameters was "turned off" during the bias processing. Similarly, in the drift orbit at orbit normal attitude, a correlation between sensor mounting angle and Earth sensor triggering biases necessitated that a member of this pair of biases be turned off. For this geometry a correlation also existed between the sensor azimuth biases and the in-track orbit timing error, requiring that one of these parameters (usually the latter) be turned off.

The subsystem used to determine the biases for the sensor hardware during the CTS mission was OABIAS. Although OABIAS is capable of operation in both a differential correction and a recursive mode, only the former mode was used because prelaunch analysis had indicated that this mode was least sensitive to a priori values of the state vector parameters. The capability of the new OABIAS system to constrain the horizon-in value to be equal to the horizon-out value for both the azimuth-level and triggering-level biases was used extensively. The quality of the OABIAS solution was checked by using plots of residuals from the OABIAS subsystem (Figure 3-9) and plots of predicted data versus observed data from the PLOTOC subsystem (Figure 3-10).

Figure 3-9 shows an example of the residual for the midscan dihedral model solution for the east Earth sensor for CTS mission data. The residual plot represents the difference between the observed Earth midscan angle and the predicted midscan angle for each frame of data processed, and it is the square of this quantity which the OABIAS system is attempting to minimize for each iteration. This particular plot indicates evidence of a systematic error which increases towards the end of the data pass. Sources of this error could be poor geometry, pagoda effect, or certain biases being "turned off" for this processing run.

In Figure 3-10 the full ellipse of "+" signs are the observed rotation angles for the west Earth sensor where the lower curve represents the horizon-in and the upper curve the horizon-out rotation angles. The partial ellipse of "+" signs

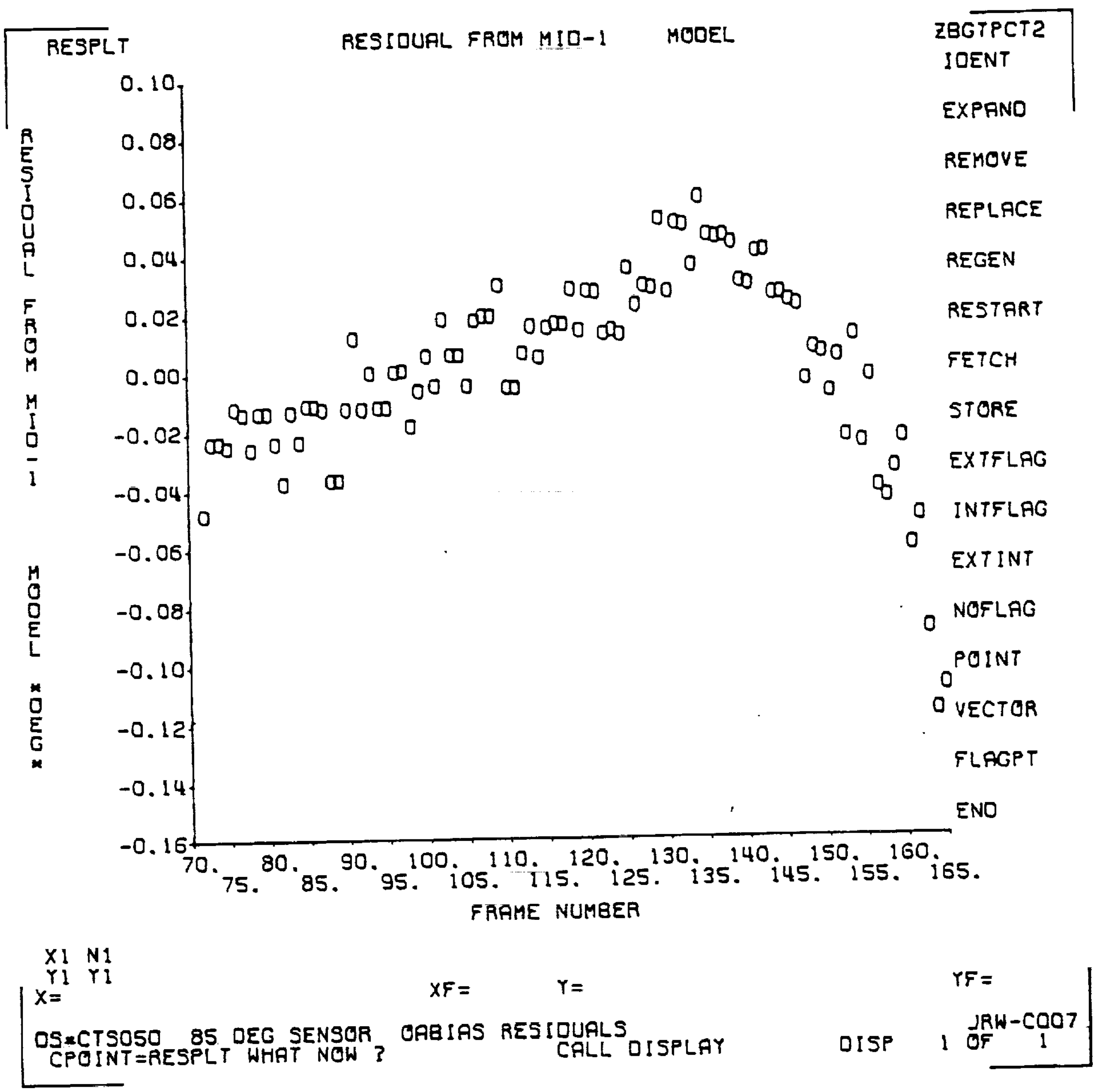


Figure 3-9. Residuals From Midscan Dihedral Model for East Earth Sensor From OABIAS

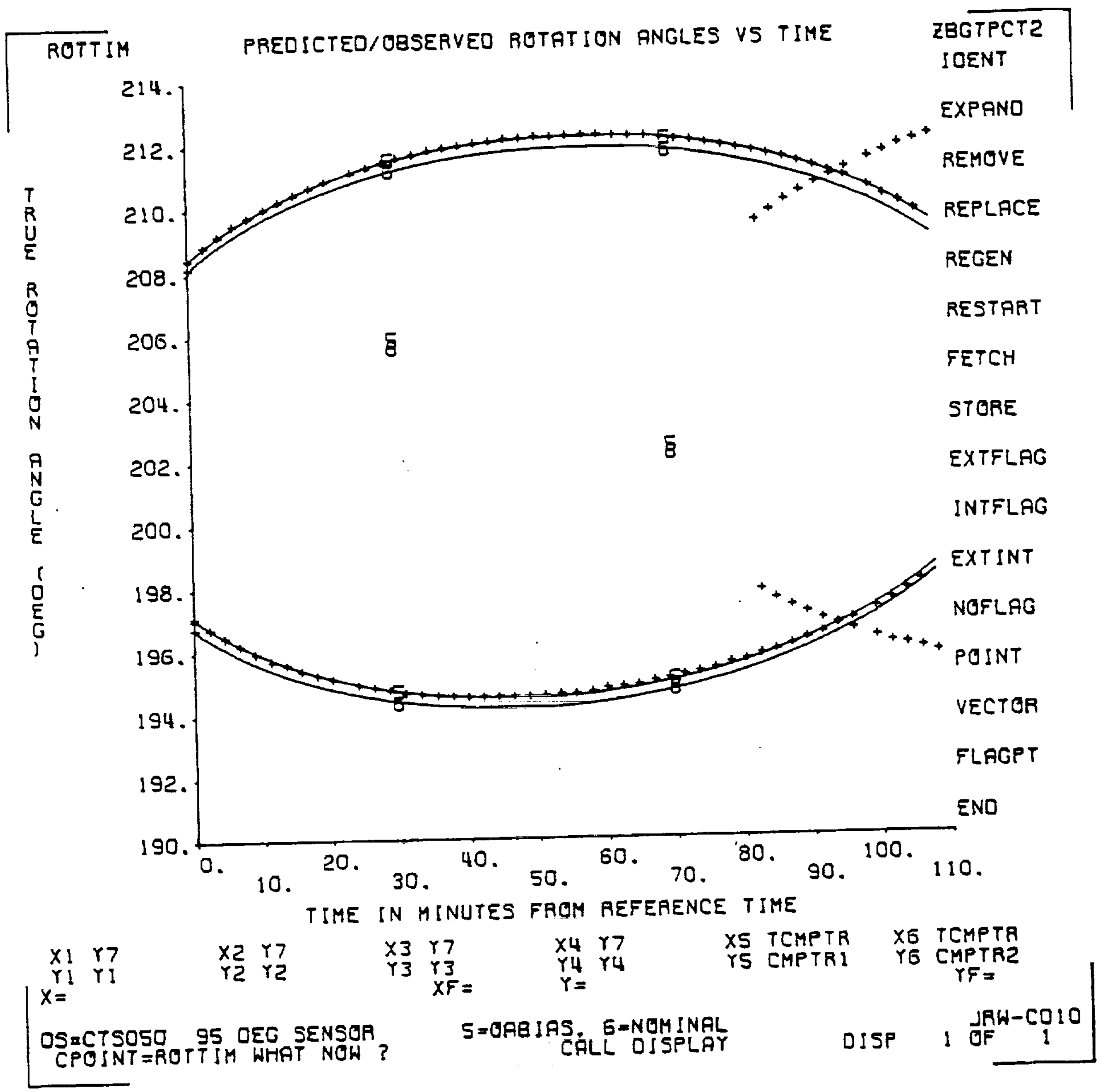


Figure 3-10. Predicted/Observed Rotation Angles Versus Time for SES-W at First Apogee for Nominal Alignment and OABIAS-Determined Biases

are the observed rotation angles for the east Earth sensor which were not processed for this run. The pair of solid lines labeled "5" denote the predicted rotation angles using the spinning sensor biases determined by the OABIAS subsystem. The pair of solid lines labeled "6" were calculated using the final prelaunch measured alignment data for the spinning attitude sensors (see Section 2). The OABIAS solution (curve 5) clearly gives an excellent fit to the data.

### 3.4.2 Summary of Sensor Biases

The history of the spinning attitude sensor biases as determined for CTS are given in Table 3-1. All biases were small and within the specified accuracy of the alignment data for the sensors and the known unmodeled errors (pagoda effect, Earth oblateness, Earth atmospheric height, orbit errors).

## Table 3-1. History of Bias Determination Results

| GMT SPAN (HH:MM) | DAY (1976) | DATA TYPE | RIGHT ASCENSION (DEGREES) | DECLINATION (DEGREES) | $\Delta\mu$ (DEGREES) | SENSOR 1* | | | | | SENSOR 2* | | | | | $\Delta t$ (SECONDS) | |
|---|---|---|---|---|---|---|---|---|---|---|---|---|---|---|---|---|---|
| | | | | | | $\gamma_1$ | $\Delta\phi_1^I$ | $\Delta\phi_1^O$ | $\Delta\rho_1^I$ | $\Delta\rho_1^O$ | $\gamma_2$ | $\Delta\phi_2^I$ | $\Delta\phi_2^O$ | $\Delta\rho_2^I$ | $\Delta\rho_2^O$ | | |
| 3:40 TO 6:46 | 1/18 | $A_1$ | 197.52 | −22.53 | −0.08 | 0.055 | −0.34 | −0.34 | 0.03 | 0.03 | 0.055 | −0.35 | −0.35 | 0.02 | 0.02 | | TRANSFER ORBIT |
| 7:51 TO 15:10 | 1/19 | $A_4 + P_4$ | 197.96 | −10.80 | 0.15 | −0.055 | −0.14 | −0.14 | 0.055 | 0.055 | −0.16 | −0.24 | −0.24 | 0.0 | 0.0 | − 6 | |
| 21:40 TO 6:20 | 1/19<br>1/20 | $A_5 + P_6$ | 17.27 | −21.94 | −0.03 | −0.07 | −0.09 | −0.09 | 0.005 | 0.005 | 0.05 | −0.17 | −0.17 | 0.003 | 0.003 | | |
| 8:46 TO 11:49 | 1/20 | $A_6$** | 17.27 | −23.42 | −0.29 | −0.02 | −0.29 | −0.29 | −0.07 | −0.07 | −0.02 | −0.25 | −0.25 | −0.02 | −0.02 | −165 | |
| 8:46 TO 15:50 | 1/20 | $A_6 + P_7$ | 17.42 | −23.19 | −0.08 | −0.02 | −0.06 | −0.06 | −0.01 | −0.01 | −0.09 | −0.1 | −0.1 | −0.03 | −0.03 | 108 | |
| 20:45 TO 16:11 | 1/21<br>1/22 | $D/O_2$ | 13.2 | −88.8 | −0.21 | −0.03 | −0.18 | −0.18 | −0.01 | −0.01 | 0.04 | −0.23 | −0.23 | −0.03 | −0.03 | | DRIFT ORBIT |
| 20:15 TO 12:52 | 1/22<br>1/23 | $D/O_3$ | 5.54 | −88.73 | −0.17 | −0.03 | −0.18 | −0.18 | −0.01 | −0.01 | 0.03 | −0.24 | −0.24 | −0.03 | −0.03 | | |
| 12:20 TO 0.18 | 1/23<br>1/26 | $D/O_{4,5}$ | 5.56 | −88.72 | −0.13 | −0.02 | −0.18 | −0.18 | −0.01 | −0.01 | 0.04 | −0.23 | −0.23 | −0.03 | −0.03 | | |
| 20:06 TO 12:12 | 1/26<br>1/27 | $D/O_7$ | 4.23 | −88.67 | −0.08 | −0.01 | −0.19 | −0.19 | −0.01 | −0.01 | 0.07 | −0.23 | −0.23 | −0.03 | −0.03 | | |
| 7:11 TO 12:18 | 1/29<br>1/29 | $D/O_8$ | 6.71 | −88.64 | −0.10 | −0.01 | −0.19 | −0.19 | −0.01 | −0.01 | 0.07 | −0.23 | −0.23 | −0.03 | −0.03 | | |

*PARAMETERS ARE EXPRESSED IN DEGREES.
**A SINUSOIDAL RESIDUAL OF 0.05 DEGREE (0.1 DEGREE WITH NO IN-TRACK CORRECTION) INDICATED A SYSTEMATIC ERROR IN THE ORBIT USED TO PROCESS THIS DATA.

KEY:

$A_n, P_n$ = APOGEE$_n$, PERIGEE$_n$

$D/O_n$ = DRIFT ORBIT$_n$

$\gamma_1, \gamma_2$ = MOUNTING ANGLES FOR SENSORS 1 AND 2, RESPECTIVELY

$\Delta\phi_1^I / \Delta\phi_1^O$, $\Delta\phi_2^I / \Delta\phi_2^O$ = AZIMUTH BIASES FOR SENSORS 1 AND 2, RESPECTIVELY

$\Delta\rho_1^I / \Delta\rho_1^O$, $\Delta\rho_2^I / \Delta\rho_2^O$ = ANGULAR EARTH RADIUS BIASES FOR SENSORS 1 AND 2 RESPECTIVELY

I/O = IN/OUT EARTH-CROSSING DATA

## SECTION 4 - ATTITUDE RESULTS

A number of discrete phases may be distinguished for the CTS mission when the spacecraft was not being maneuvered. During these periods large spans of data were collected while the spacecraft's spin axis vector remained nearly invariant in the geocentric inertial coordinate system. These phases were as follows:

- Transfer orbit
  - Injection attitude
  - System verification attitude
  - Apogee motor firing attitude (prior to trim)
  - Apogee motor firing attitude (following trim)
- Drift orbit
  - Post-apogee motor firing attitude
  - Drift orbit normal attitude (prior to first orbit maneuver)
  - Drift orbit normal attitude (prior to second orbit maneuver)
  - Drift orbit normal attitude (prior to third orbit maneuver)
  - Drift orbit normal attitude (prior to fourth orbit maneuver)
  - Drift orbit normal attitude (prior to fifth (final) orbit maneuver)
  - Drift orbit normal attitude (after fifth (final) orbit maneuver)

The attitude history and corresponding orbit information for these discrete phases are listed in Table 4-1 and Table 4-2, respectively. Successive orbit trim maneuvers following the second orbit maneuver had little effect on the spacecraft's attitude.

An upper limit on the arc-length uncertainty for the attitude results for CTS was conservatively fixed at 0.5 degree. This value was supported by arc-length uncertainty results determined by the Optical Aspect Attitude Determination System (OASYS) (using a priori alignment data) and by the sensor biases determined by OABIAS being no larger than approximately one-third degree.

Table 4-1. CTS Attitude History

| ATTITUDE SOLUTION | COMMENT | INTERVAL[1] (GMT) | | | | SPIN AXIS | | SPIN RATE (RPM) | SUN ANGLE[2] (DEGREES) |
|---|---|---|---|---|---|---|---|---|---|
| | | FROM | | TO | | | | | |
| | | YY/MM/DD | HH:MM | YY/MM/DD | HH:MM | RIGHT ASCENSION (DEGREES) | DECLINATION (DEGREES) | | |
| 1 | PRIOR TO REORIENTATION TO SVA | 76/01/17 | 23:52 | 76/01/19 | 03:28 | 197.52 | −22.53 | 61.7 | 92.9 |
| 2 | AT SVA | 76/01/19 | 03:30 | 76/01/19 | 23:08 | 198.08 | −10.96 | 61.7 | 97.9 |
| 3 | PRIOR TO AMFA TRIM | 76/01/20 | 00:16 | 76/01/20 | 08:45 | 17.27 | −21.94 | 61.0 | 70.1 |
| 4 | PRIOR TO AMF (AFTER AMF TRIM) | 76/01/20 | 08:46 | 76/01/20 | 20:40 | 17.48 | −23.20 | 61.0 | 69.6 |
| 5 | PRIOR TO REORIENTATION TO NEGATIVE ORBIT NORMAL (AFTER AMF) | 76/01/20 | 20:42 | 76/01/20 | 22:40 | 17.28 | −23.43 | 61.1 | 69.1 |
| 6 | PRIOR TO FIRST ORBIT MANEUVER | 76/01/20 | 23:20 | 76/01/21 | 06:11 | 15:80 | −88.82 | 61.1 | 69.6 |
| 7 | PRIOR TO SECOND ORBIT MANEUVER | 76/01/21 | 20:45 | 76/01/22 | 16:11 | 13.20 | −88.80 | 60.8 | 69.9 |
| 8 | AFTER SECOND ORBIT MANEUVER | 76/01/22 | 20:15 | 76/01/23 | 12:52 | 5.54 | −88.73 | 60.3 | 69.9 |
| 9 | PRIOR TO THIRD ORBIT MANEUVER | 76/01/23 | 12:20 | 76/01/26 | 00:18 | 5.56 | −88.72 | 60.3 | 70.1 |
| 10 | AFTER THIRD ORBIT MANEUVER | 76/01/26 | 20:06 | 76/01/27 | 12:12 | 4.23 | −88.67 | 60.0 | 70.6 |
| 11 | AFTER FOURTH ORBIT MANEUVER | 76/01/28 | 07:12 | 76/01/28 | 12:19 | 5.64 | −88.64 | 59.9 | 70.9 |
| 12 | AFTER FIFTH (FINAL) ORBIT MANEUVER | 76/01/29 | 07:11 | 76/01/29 | 12:19 | 6.71 | −88.64 | 59.9 | 71.1 |

[1]TIME GAPS INDICATE THE OCCURRENCE OF ATTITUDE OR ORBIT MANEUVERS.

[2]THE SUN ANGLES ARE APPROXIMATELY AT THE MIDDLE OF THE INTERVAL.

Table 4-2. Orbit Information Corresponding to Attitude History

| ATTITUDE SOLUTION | SEMIMAJOR AXIS (KILOMETERS) | ECCENTRICITY | INCLINATION (DEGREES) | MEAN ANOMALY (DEGREES) | ARGUMENT OF PERIGEE (DEGREES) | ASCENDING NODE (DEGREES) | EPOCH (GMT) | |
|---|---|---|---|---|---|---|---|---|
| | | | | | | | YY/MM/DD | HH:MM:SS |
| 1 | 24579.1 | 0.733086 | 27.2013 | 0.439642 | 178.824 | 288.005 | 76/01/17 | 23:52:00 |
| 2 | 24481.9 | 0.731987 | 27.1817 | 219.667 | 179.506 | 287.598 | 76/01/19 | 03:30:00 |
| 3 | 24491.3 | 0.731189 | 27.2894 | 207.287 | 180.075 | 287.261 | 76/01/20 | 00:19:00 |
| 4 | 24491.6 | 0.73119 | 27.29 | 207.29 | 180.08 | 287.26 | 76/01/20 | 00:19:00 |
| 5 | 41339.4 | 0.025534 | 0.713824 | 210.553 | 203.487 | 267.169 | 76/01/20 | 22:52:56 |
| 6 | 41296.7 | 0.026776 | 0.683701 | 206.096 | 209.573 | 265.342 | 76/01/20 | 22:52:56 |
| 7 | 41436.1 | 0.023323 | 0.680755 | 179.886 | 209.801 | 265.248 | 76/01/21 | 20:24:00 |
| 8 | 41990.8 | 0.009867 | 0.678311 | 167.266 | 211.709 | 265.090 | 76/01/22 | 19:00:00 |
| 9 | 41992.1 | 0.009873 | 0.675660 | 52.5911 | 212.040 | 265.122 | 76/01/23 | 11:14:00 |
| 10 | 42285.3 | 0.002853 | 0.664803 | 171.131 | 213.220 | 265.148 | 76/01/26 | 18:30:00 |
| 11 | 42205.3 | 0.001074 | 0.659264 | 342.777 | −146.674 | 265.061 | 76/01/28 | 06:00:00 |
| 12 | 42167.4 | 0.000187 | 0.655530 | 347.200 | −135.429 | 264.906 | 76/01/29 | 07 00:00 |

Low residuals (0.15 degree) from OABIAS also indicated that the observed data had been satisfactorily modeled.

# SECTION 5 - CONTROL SYSTEM PERFORMANCE

The Ax HTE was used to perform all attitude reorientations, and it performed well. Through the effective use of the control monitor subsystem, all attitude reorientation maneuvers were completed within 1 degree of the desired attitude; as a result, only a 1-degree trim maneuver was needed prior to AMF, and no trim maneuver was required to achieve DONA. In the subsections which follow, each attitude maneuver will be discussed briefly.

In all the plots presented in this section, the solid line represents the predicted variation during the attitude maneuver as computed by the CTS maneuver control program (CTSMAN), and the symbol "+" reoresents the observed value during the actual maneuver.

## 5.1 INJECTION ATTITUDE (INJA) TO SYSTEM VERIFICATION ATTITUDE (SVA)

Figures 5-1 and 5-2 show the observed maneuver from INJA to SVA. The predicted plot is for the full maneuver from INJA to AMFA. The first short segment of the predicted plot is for INJA to SVA and was computed for a firing of 90 pulses of the Ax HTE. In the actual maneuver, 93 pulses were fired; therefore, the observed trajectory extends beyond the predicted trajectory. Otherwise, the observed maneuver was very close to the predicted trajectory.

## 5.2 SVA TO AMFA

The maneuver from SVA to AMFA was planned to be performed in two segments in order to have the spinning Earth sensor coverage available throughout the maneuver. In Figures 5-3 through 5-11, the shorter segment of the predicted maneuver is from SVA to an intermediate attitude (INTA), and the longer segment is from INTA to AMFA.

### 5.2.1 SVA to INTA

Figures 5-3 through 5-5 show the observed maneuver from SVA to INTA. The observed trajectory is slightly off the predicted trajectory. The firing angle

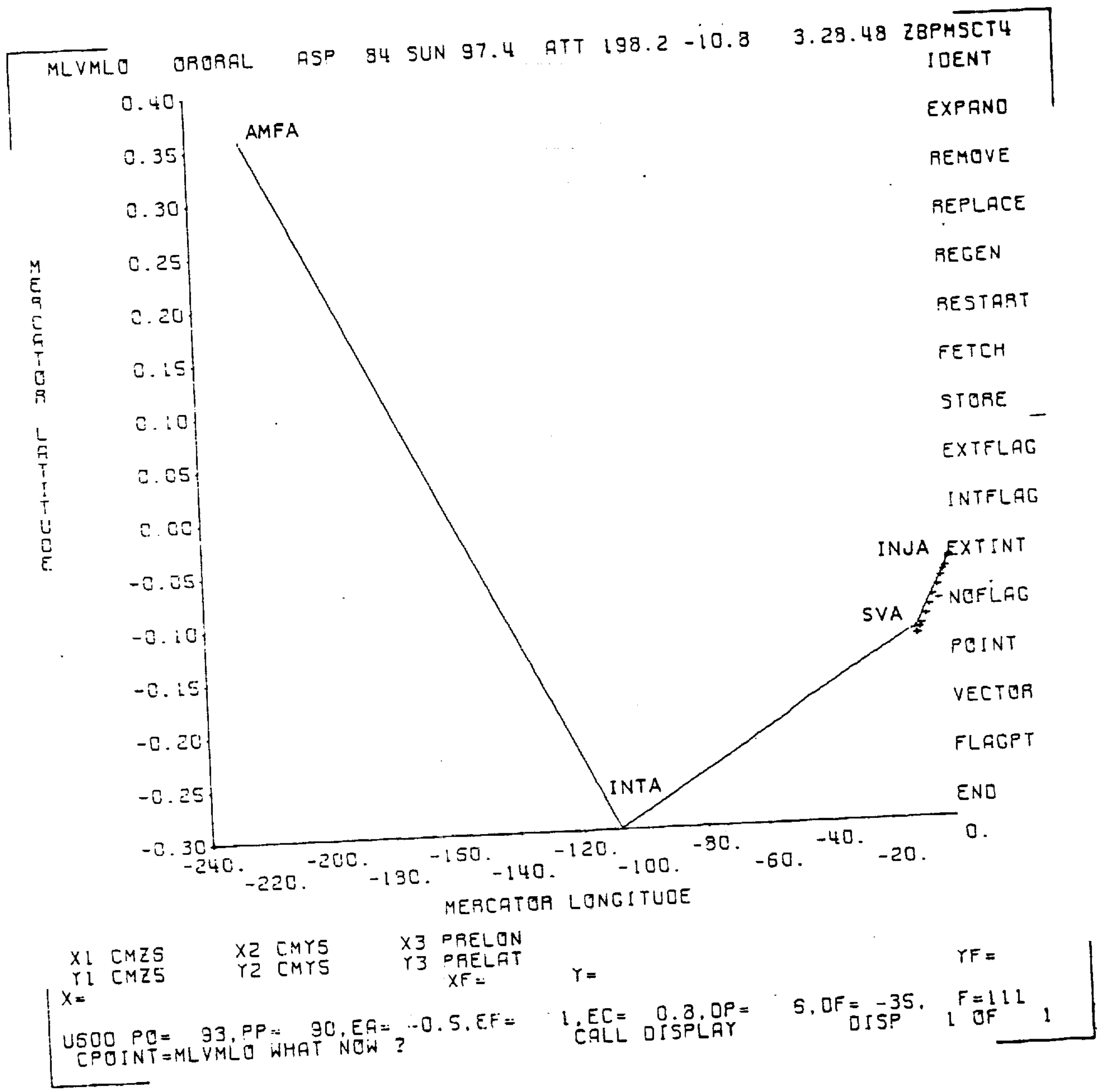


Figure 5-1. Mercator Latitude Versus Mercator Longitude Plot for Predicted Maneuver From INJA to AMFA and Observed Maneuver From INJA to SVA

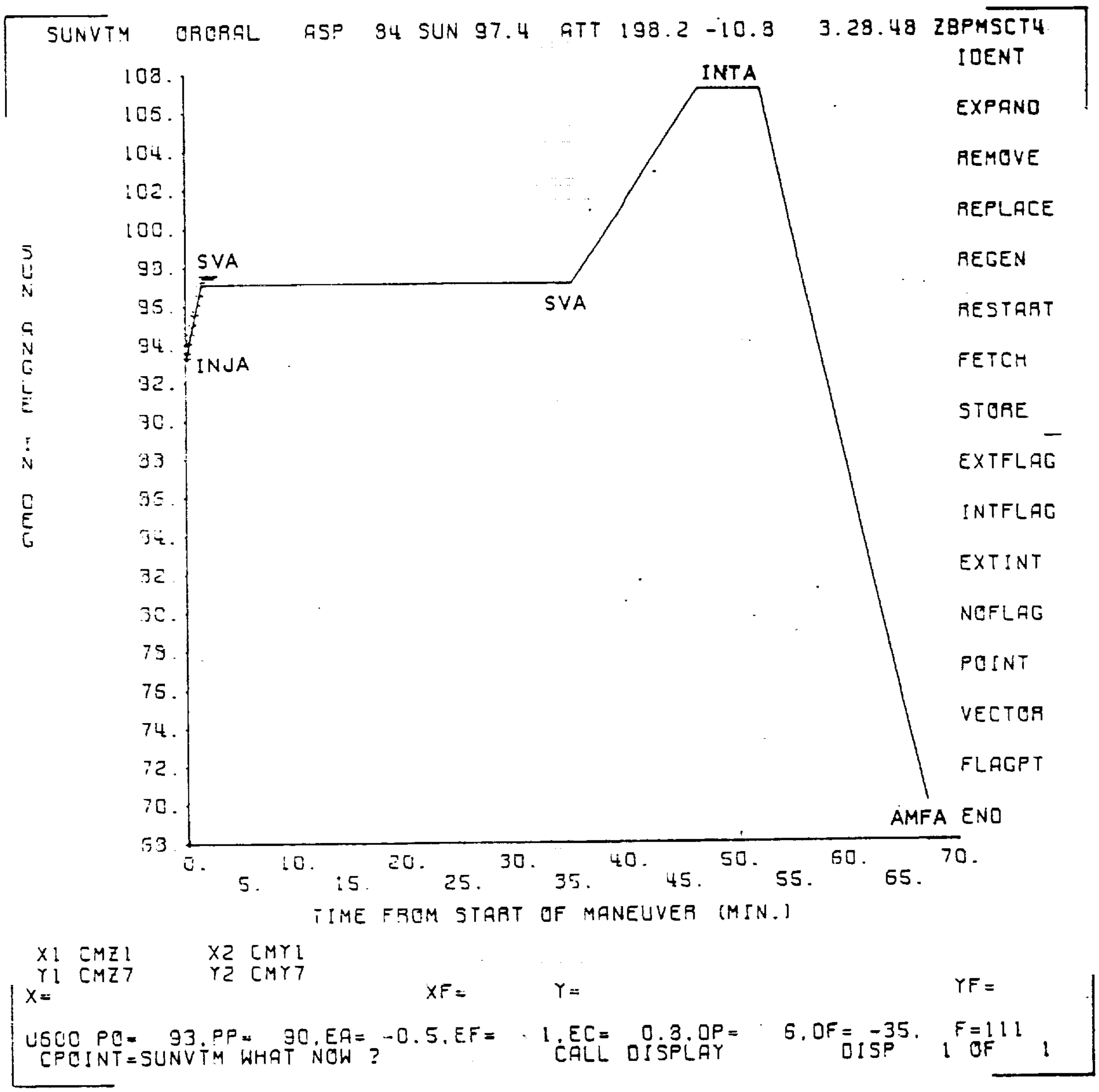


Figure 5-2. Sun Angle Versus Time Plot for Predicted Maneuver From INJA to AMFA and Observed Maneuver From INJA to SVA

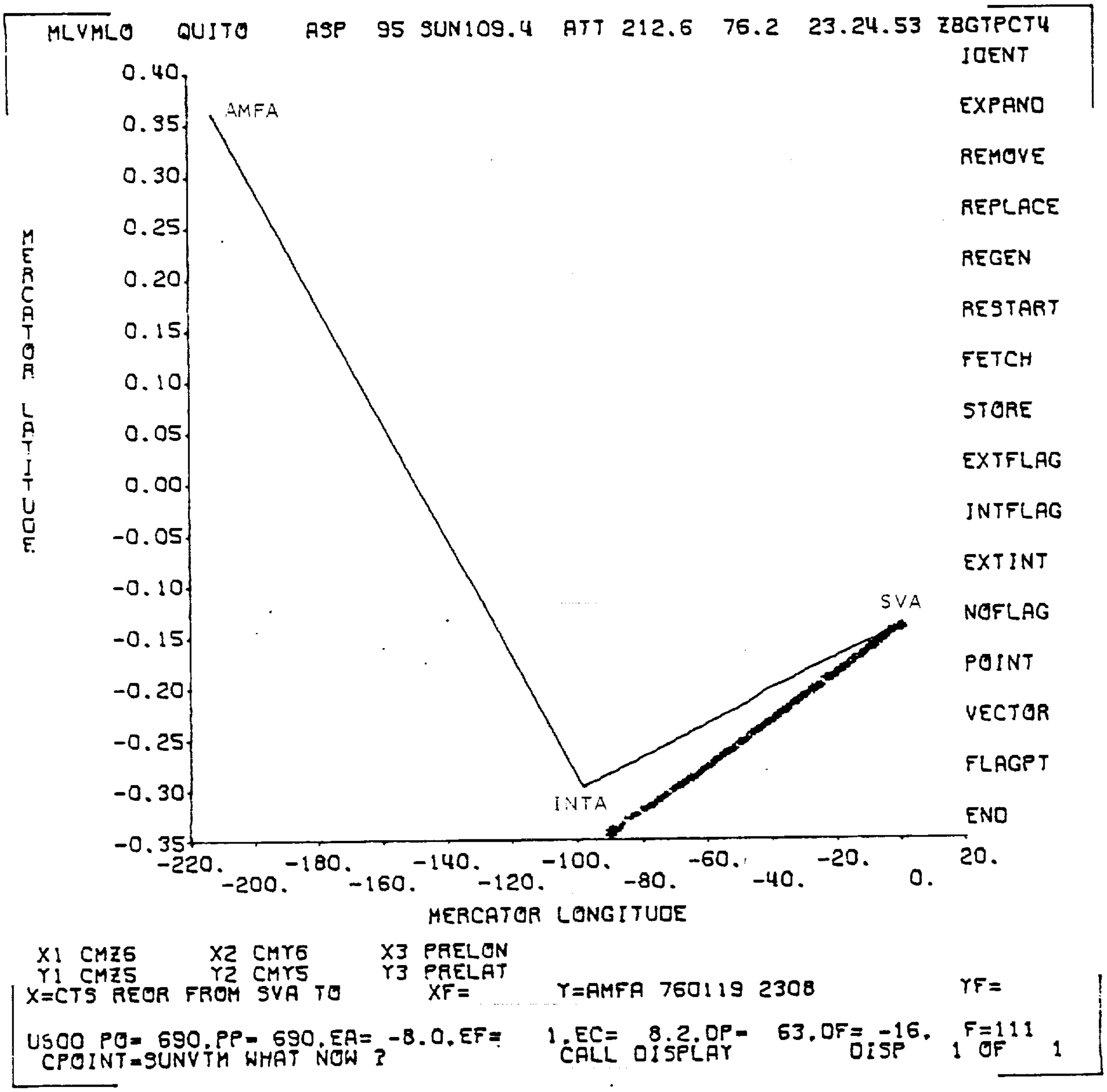


Figure 5-3. Mercator Latitude Versus Mercator Longitude Plot for Predicted Maneuver From SVA to AMFA and Observed Maneuver From SVA to INTA

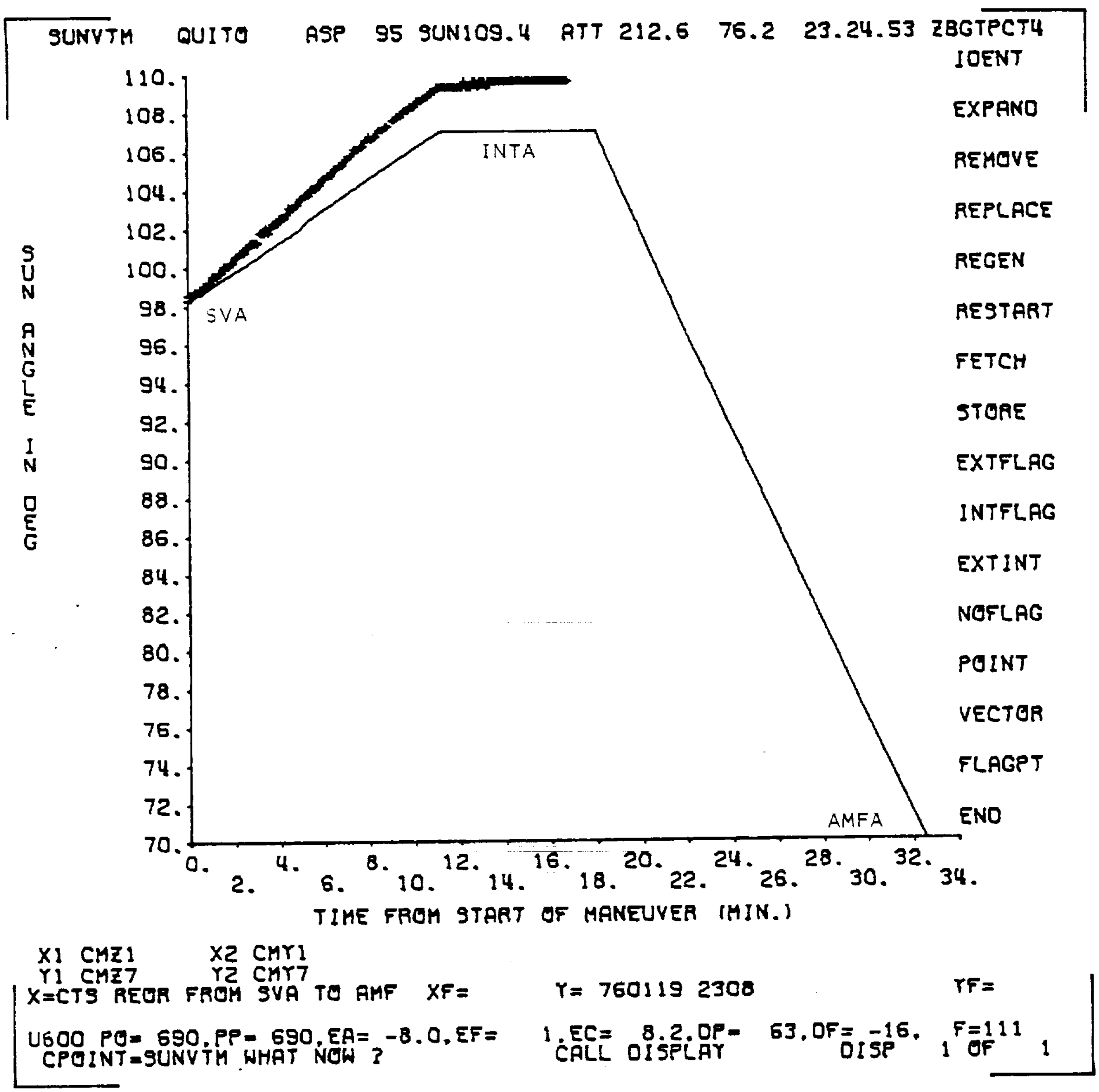


Figure 5-4. Sun Angle Versus Time Plot for Predicted Maneuver From SVA to AMFA and Observed Maneuver From SVA to INTA

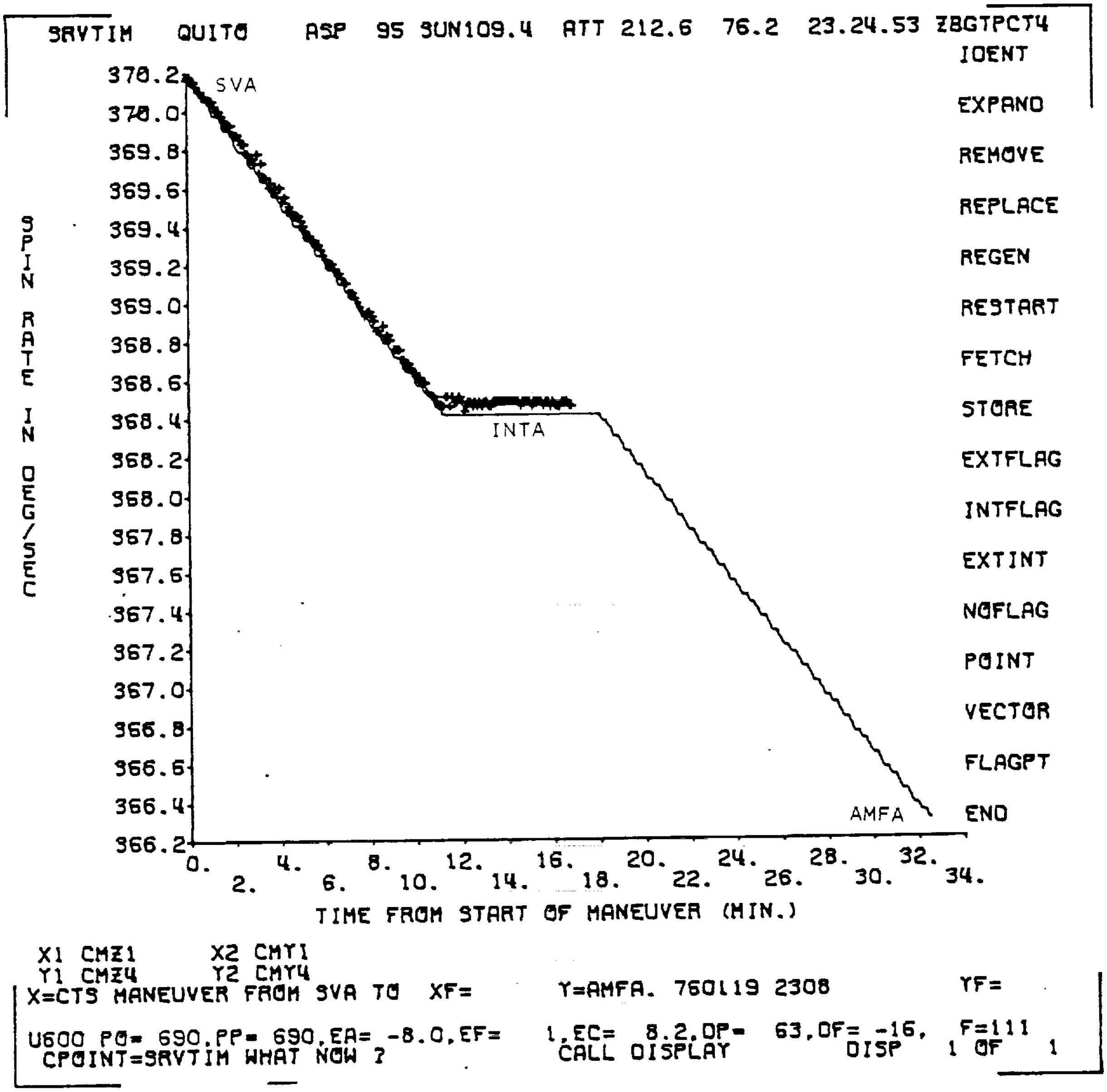


Figure 5-5. Spin Rate Versus Time Plot for Predicted Maneuver From SVA to AMFA and Observed Maneuver From SVA to INTA

error computed by the control monitor is approximately ±1.5 degrees. For this segment, 690 pulses of the Ax HTE were fired. The total rhumb line arc length traveled is about 8 percent smaller than that predicted. In Figure 5-5, it is seen that the observed spin rates are very close to the predicted values. The slightly larger observed spin rate at INTA is attributed to the fact that the total rhumb line arc length traveled is about 8 percent shorter than that predicted.

### 5.2.2 INTA to AMFA

Figures 5-6 through 5-11 show the progress of observed maneuver from INTA to AMFA. The maneuver from INTA to AMFA was stopped four times when nearing AMFA, and the firing angle was changed twice in order to achieve AMFA closely. Figure 5-6 shows the observed maneuver up to the first stop after INTA. From INTA to the first stop, 775 pulses of the Ax HTE were fired. The firing angle was changed at the first stop. Figure 5-7 includes the observed maneuver from the first stop to the third stop. In this segment a total of 186 pulses of the Ax HTE were fired in 2 groups of 93 with a short pause at the second stop. The firing angle was changed a second time at the third stop. Figure 5-8 includes the observed maneuver from the third stop to AMFA. In this segment 62 pulses of the Ax HTE were fired in 2 groups of 31 with a short pause at the fourth stop.

Figures 5-9 and 5-10 show the variation of the Sun angle and the spin rate, respectively, for the full maneuver. In these plots discontinuities followed by lines of constant Sun angle or spin rate indicate stops. Figure 5-11 is the plot of right ascension versus declination for the full maneuver. A total of 1023 pulses of the Ax HTE were fired for the maneuver from INTA to AMFA.

## 5.3 TRIM MANEUVER TO AMFA

The accurate attitude determination using a long data span after maneuver to AMFA showed that the attitude achieved was 1 degree short of the desired

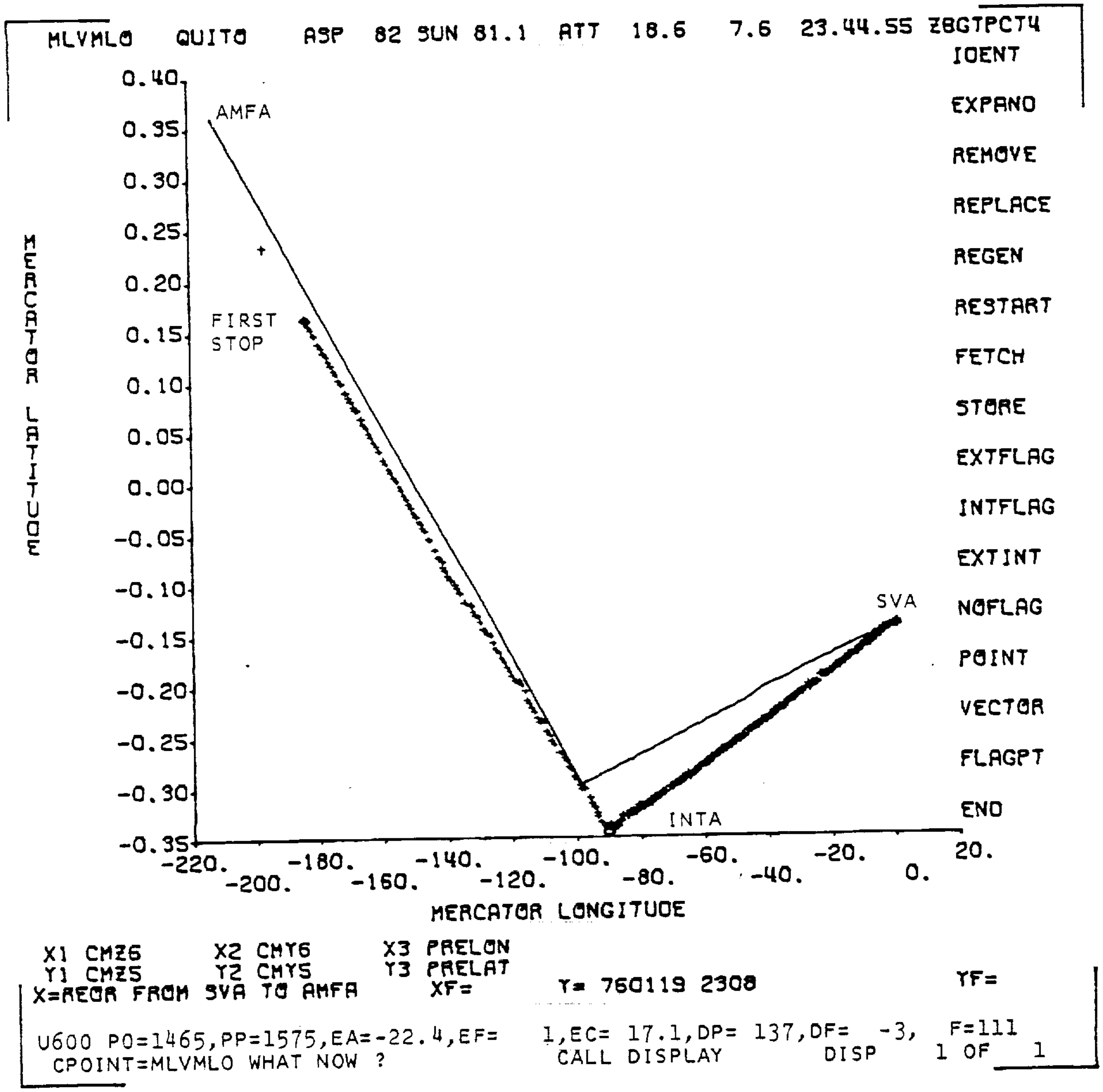


Figure 5-6. Mercator Latitude Versus Mercator Longitude Plot for Predicted Maneuver From SVA to AMFA and Observed Maneuver to First Stop After INTA (Stop at Which Firing Angle Was Changed)

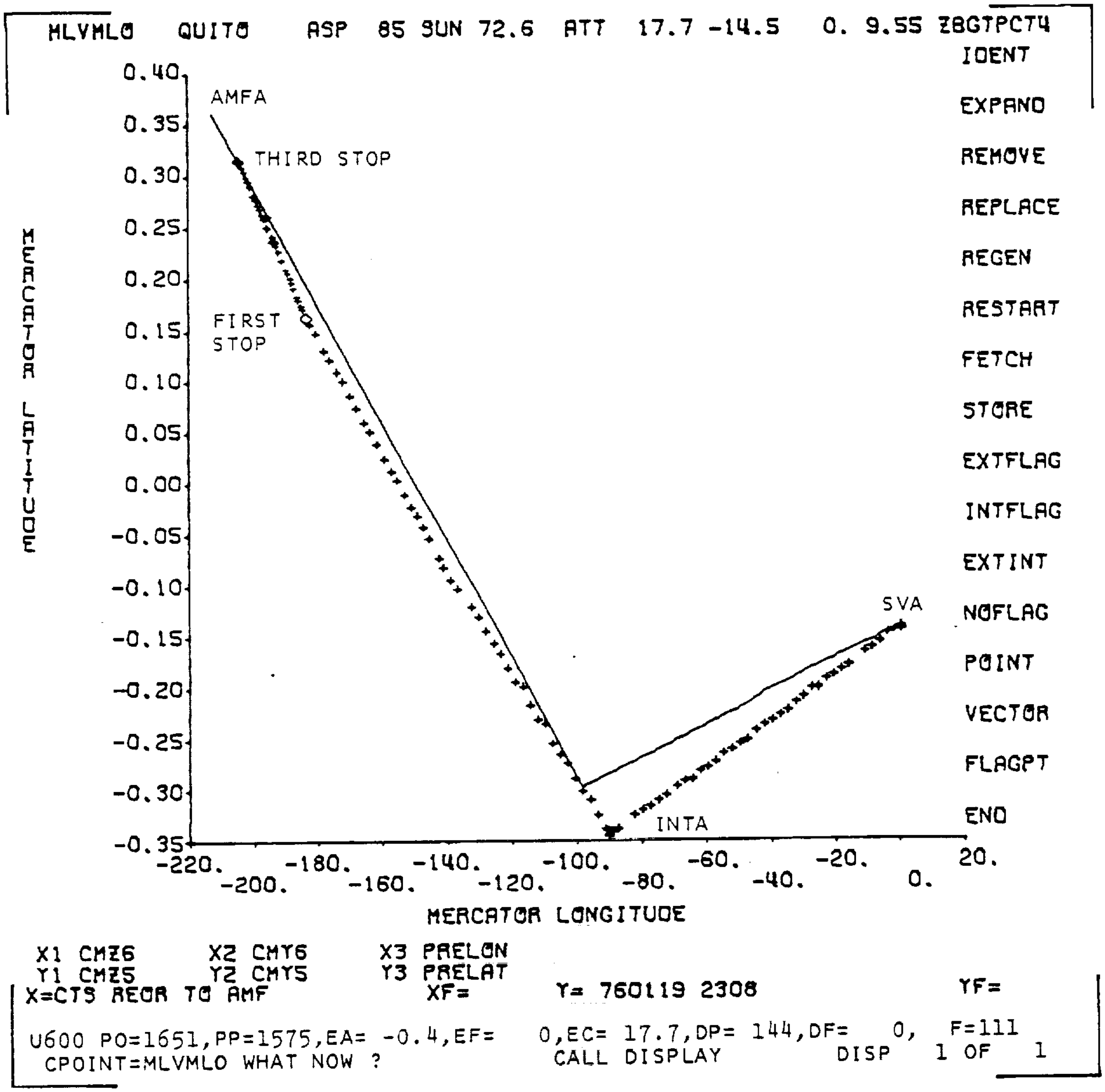


Figure 5-7. Mercator Latitude Versus Mercator Longitude Plot for Predicted Maneuver From SVA to AMFA and Observed Maneuver to Third Stop After INTA (Stop at Which Firing Angle Was Changed)

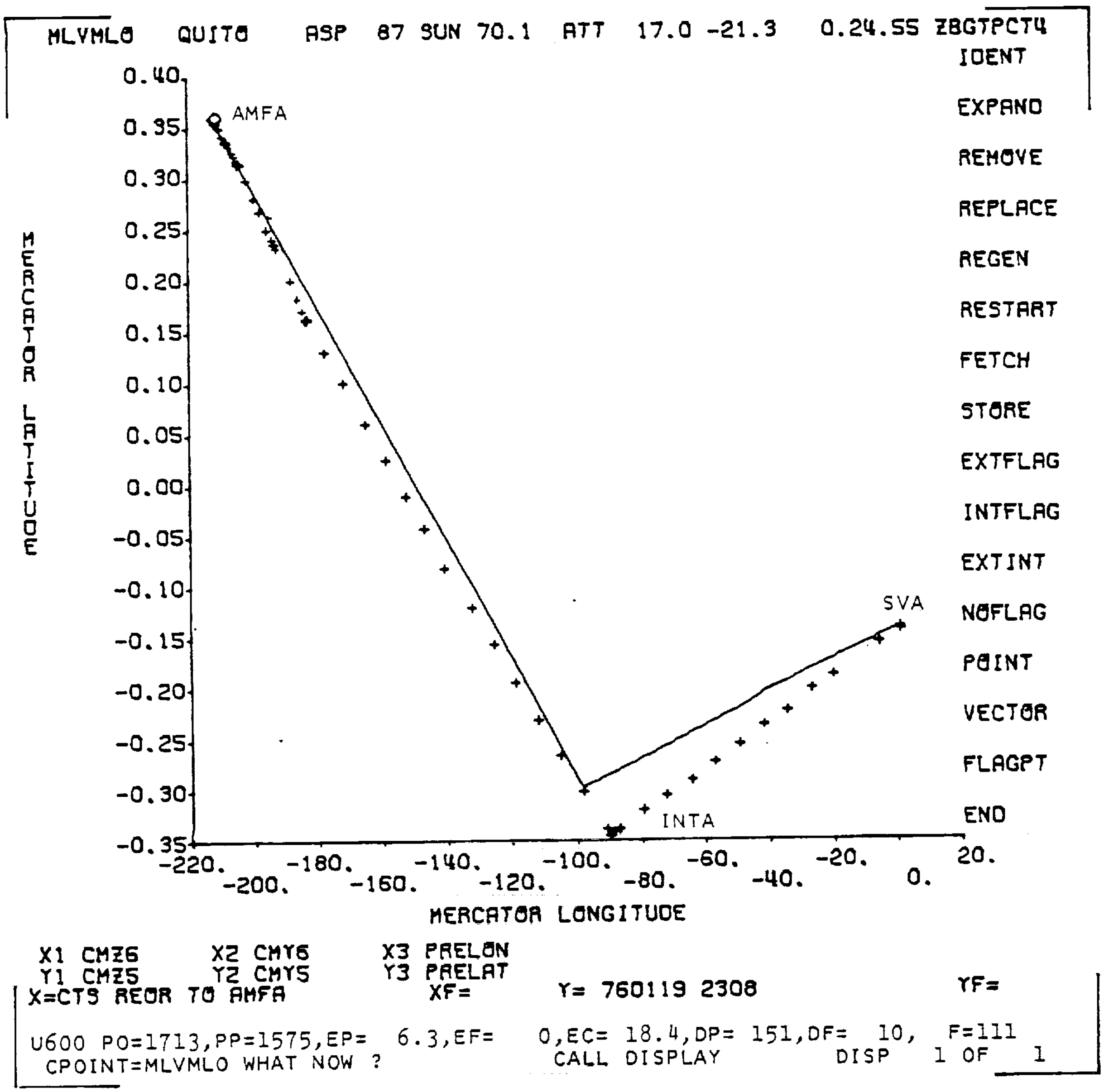


Figure 5-8. Mercator Latitude Versus Mercator Longitude Plot for Predicted and Observed Maneuvers From SVA to AMFA

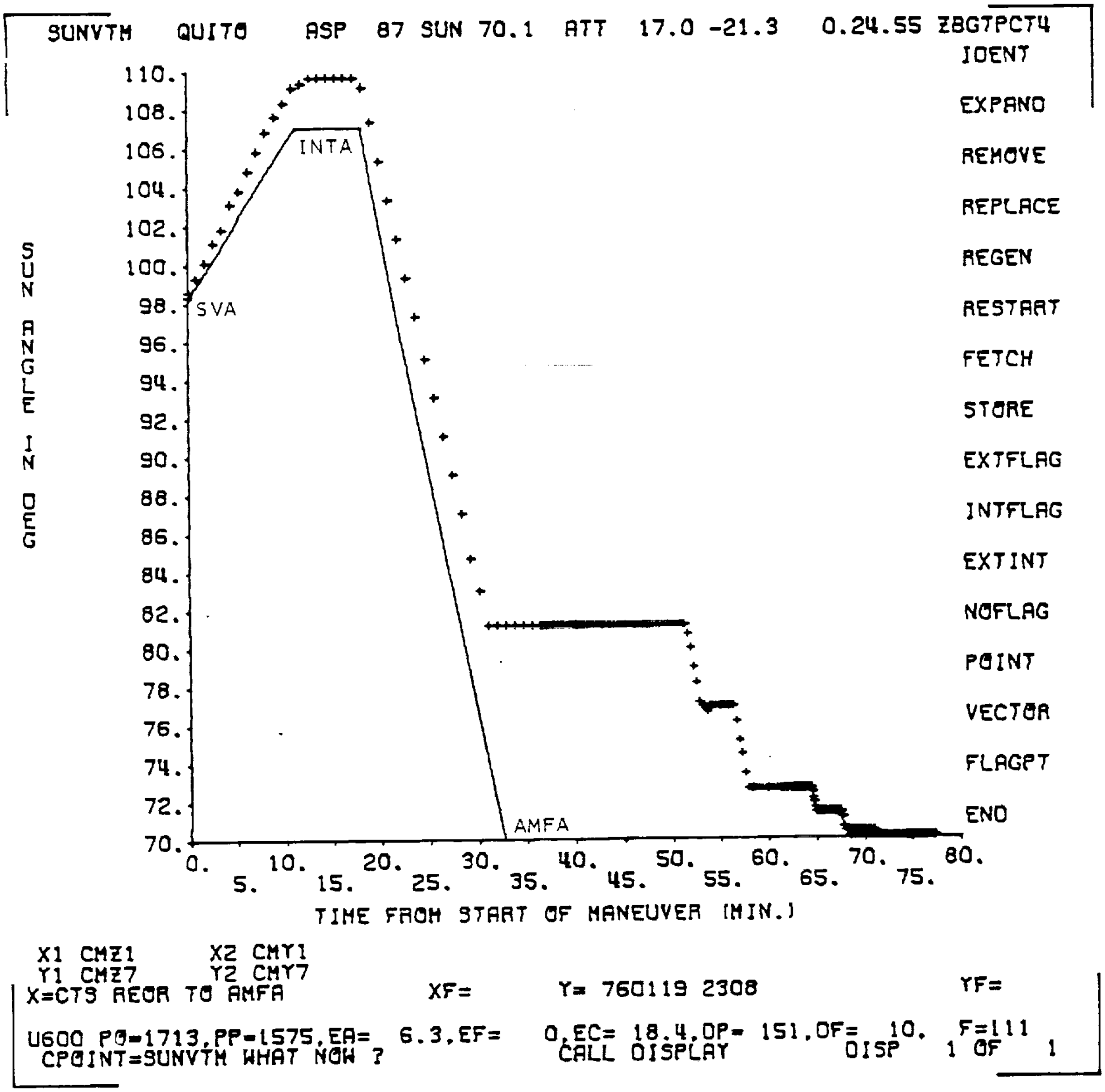


Figure 5-9. Sun Angle Versus Time Plot for Predicted and Observed Maneuvers From SVA to AMFA

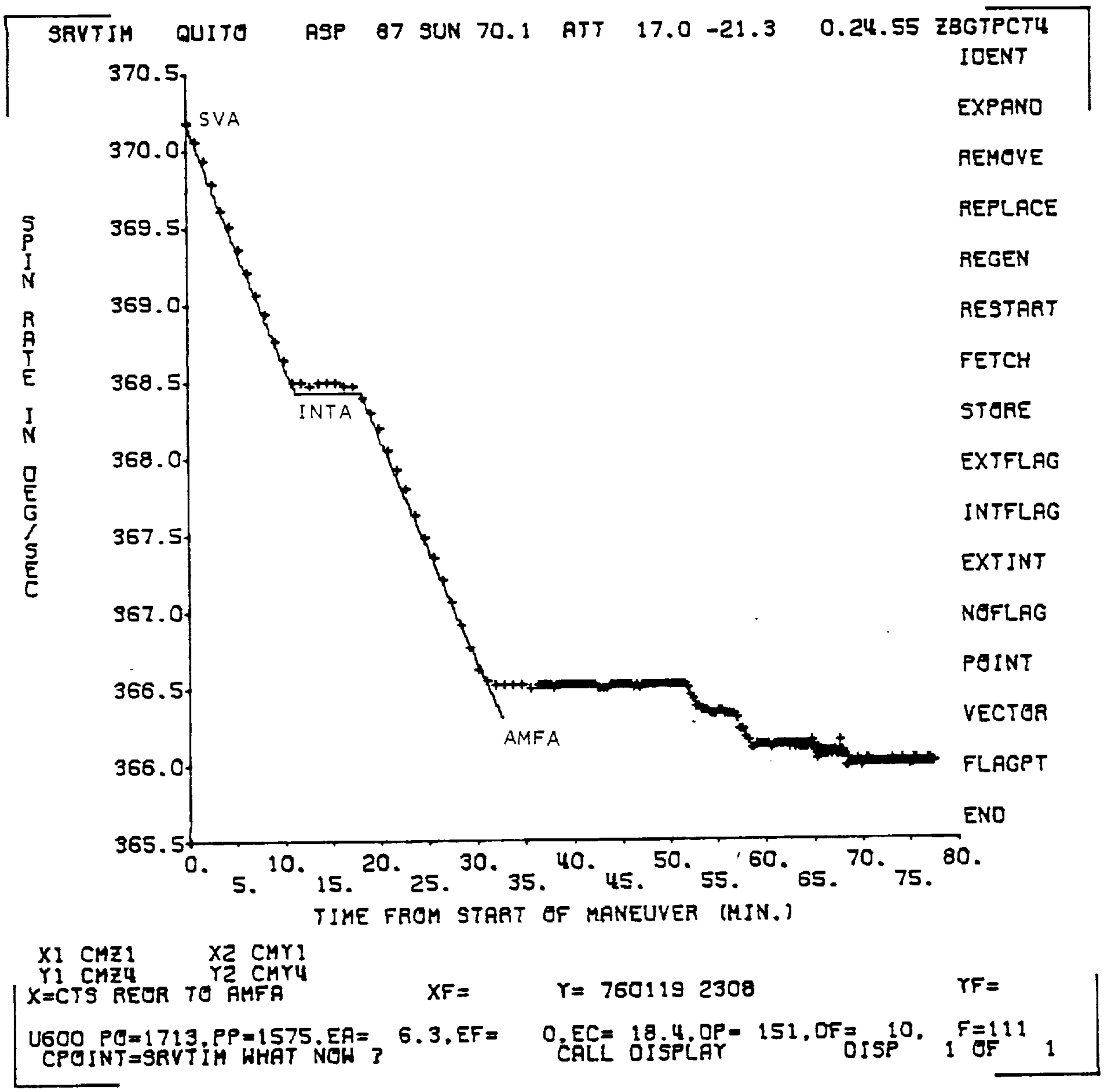


Figure 5-10. Spin Rate Versus Time Plot for Predicted and Observed Maneuvers From SVA to AMFA

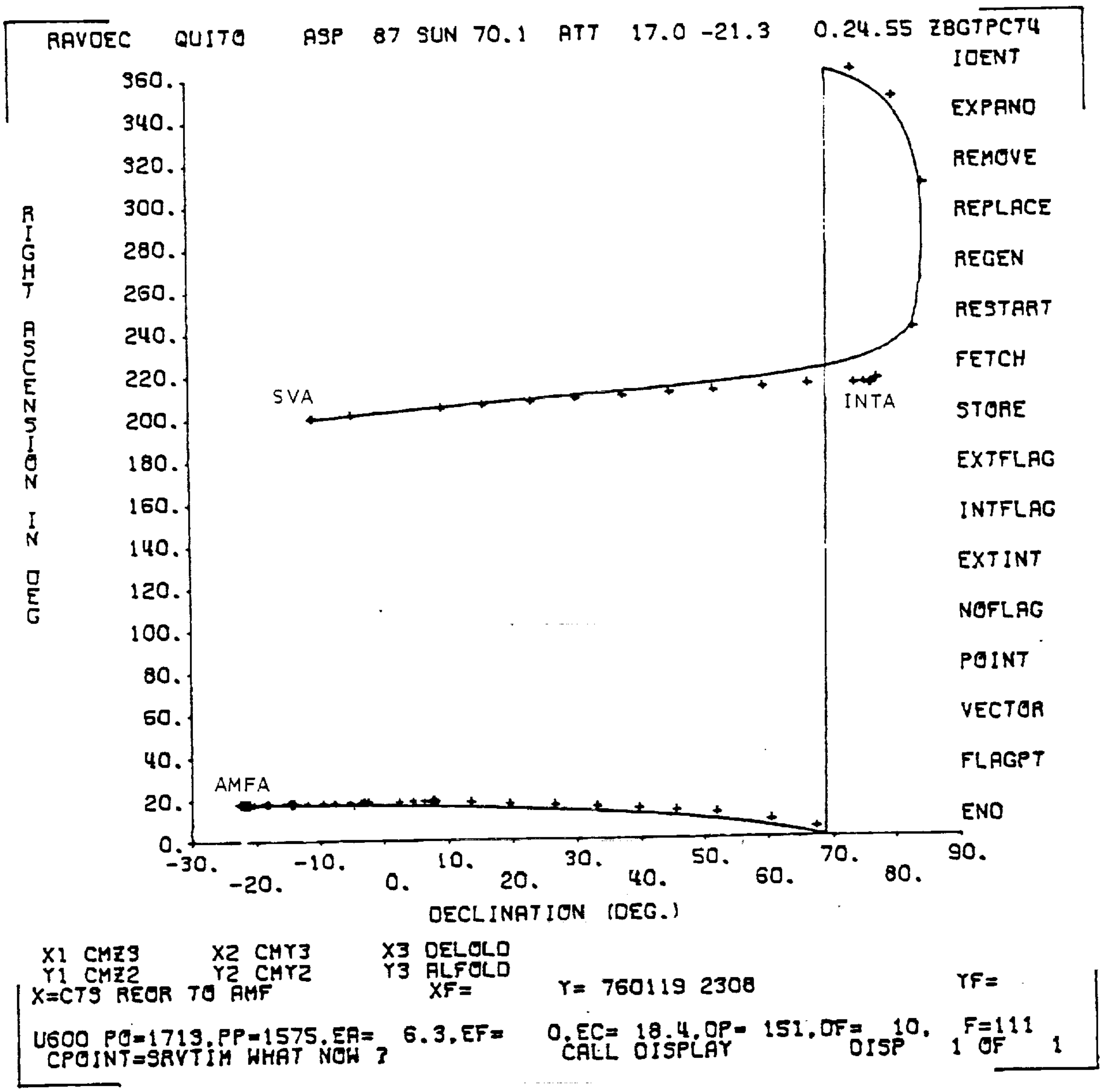


Figure 5-11. Right Ascension Versus Declination Plot for Predicted and Observed Maneuvers From SVA to AMFA

AMFA. Therefore, a trim maneuver to AMFA by firing 12 pulses of the Ax HTE was performed, and the required AMFA was achieved.

## 5.4 AMFA TO DONA

Figures 5-12 through 5-15 show the progress of observed maneuver from AMFA to DONA. This maneuver was intitiated without the spinning Earth sensor coverage, and therefore initially the Sun angle variation (Figure 5-12) was used to monitor the maneuver. About halfway through the maneuver, the Earth was picked up by the SES-W, and it was observed (Figure 5-13) that the maneuver was going slightly off the planned trajectory. It was decided to continue the maneuver until the attitude fell on the second predicted segment. This was achieved (Figure 5-14) after 434 pulses of the Ax HTE had been fired. At this point the firing angle was changed, and 62 pulses of the AX HTE were fired. It was observed that the maneuver was slightly off the planned trajectory (Figure 5-15); therefore the firing angle was changed a second time, 21 more pulses of the Ax HTE were fired, and DONA (Figure 5-15) was achieved. Accurate attitude determination using a long data span showed that the attitude achieved was within 1 degree of the DONA, and therefore a trim maneuver was not needed.

## 5.5 SUMMARY OF ATTITUDE CONTROL SYSTEM PERFORMANCE

Table 5-1 presents a history of commands executed for the attitude maneuvers and the attitudes achieved at the end of the maneuvers. The observed torque per pulse of the Ax HTE was approximately 8 percent lower than that predicted, and the observed rhumb angles of maneuvers were approximately 1.5 degrees larger than those predicted. After termination of the maneuvers, the spin rate and the Sun angle were observed to be fluctuating for a few minutes. The amplitude of fluctuation was small; it is attributed to small nutation induced due to attitude maneuvers and is consistent with the prelaunch analysis. The stabilization of the spin rate and the Sun angle in a few minutes indicates that the passive nutation damper was performing well.

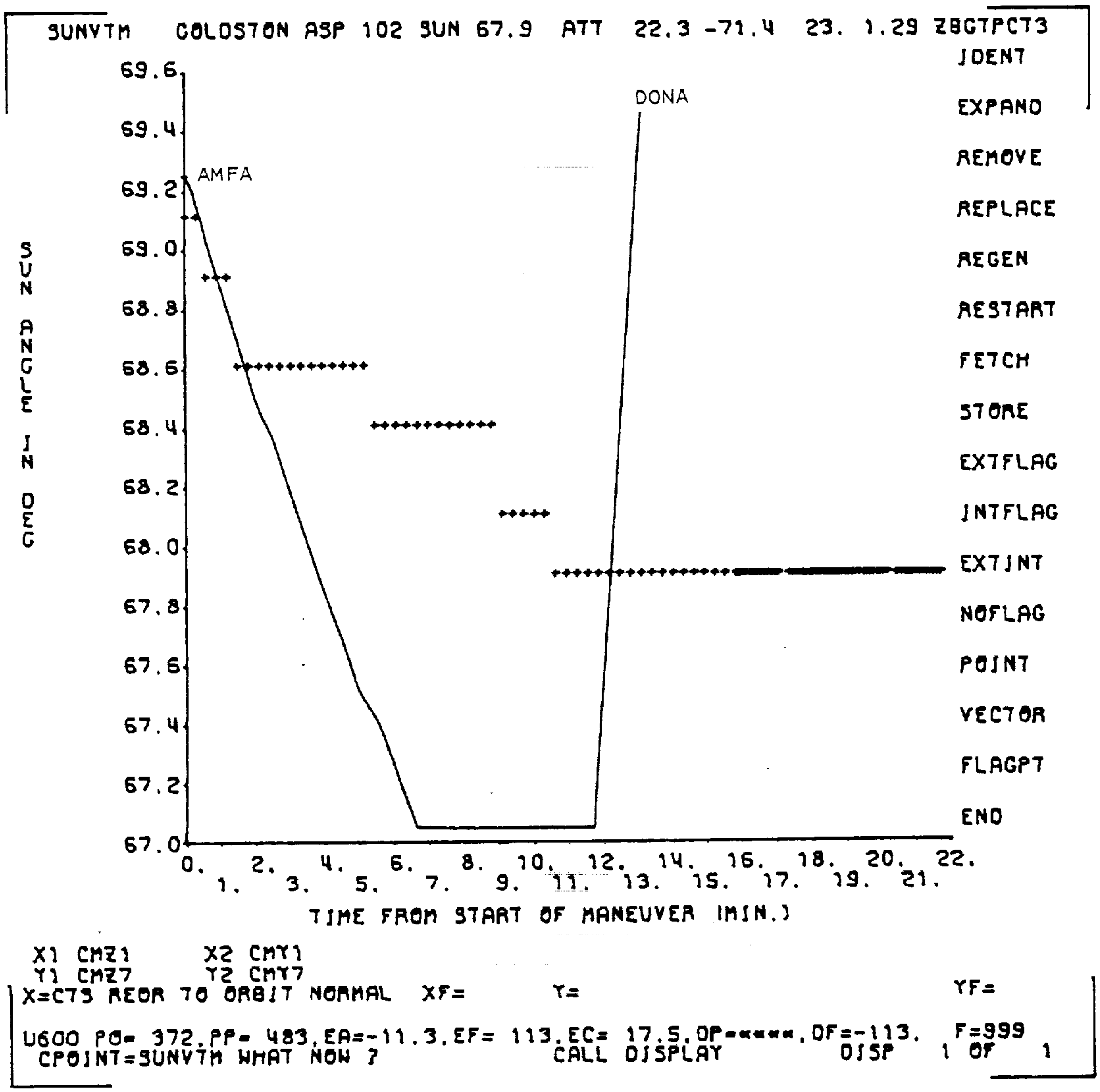


Figure 5-12. Sun Angle Versus Time Plot for Predicted Maneuver From AMFA to DONA and Observed Maneuver Prior to First Firing Angle Change

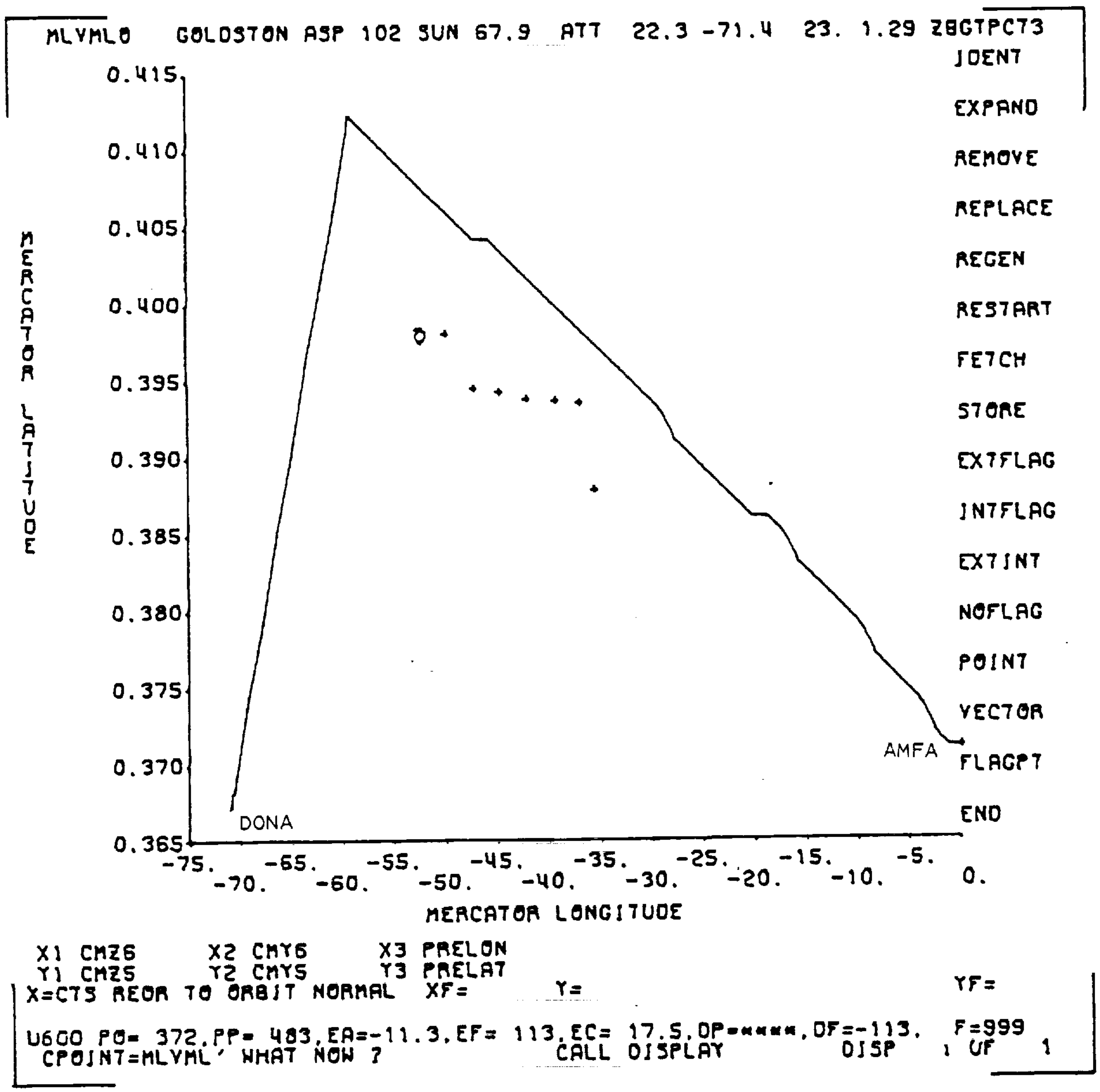


Figure 5-13. Mercator Latitude Versus Mercator Longitude Plot for Predicted Maneuver From AMFA to DONA and Observed Maneuver Prior to First Firing Angle Change

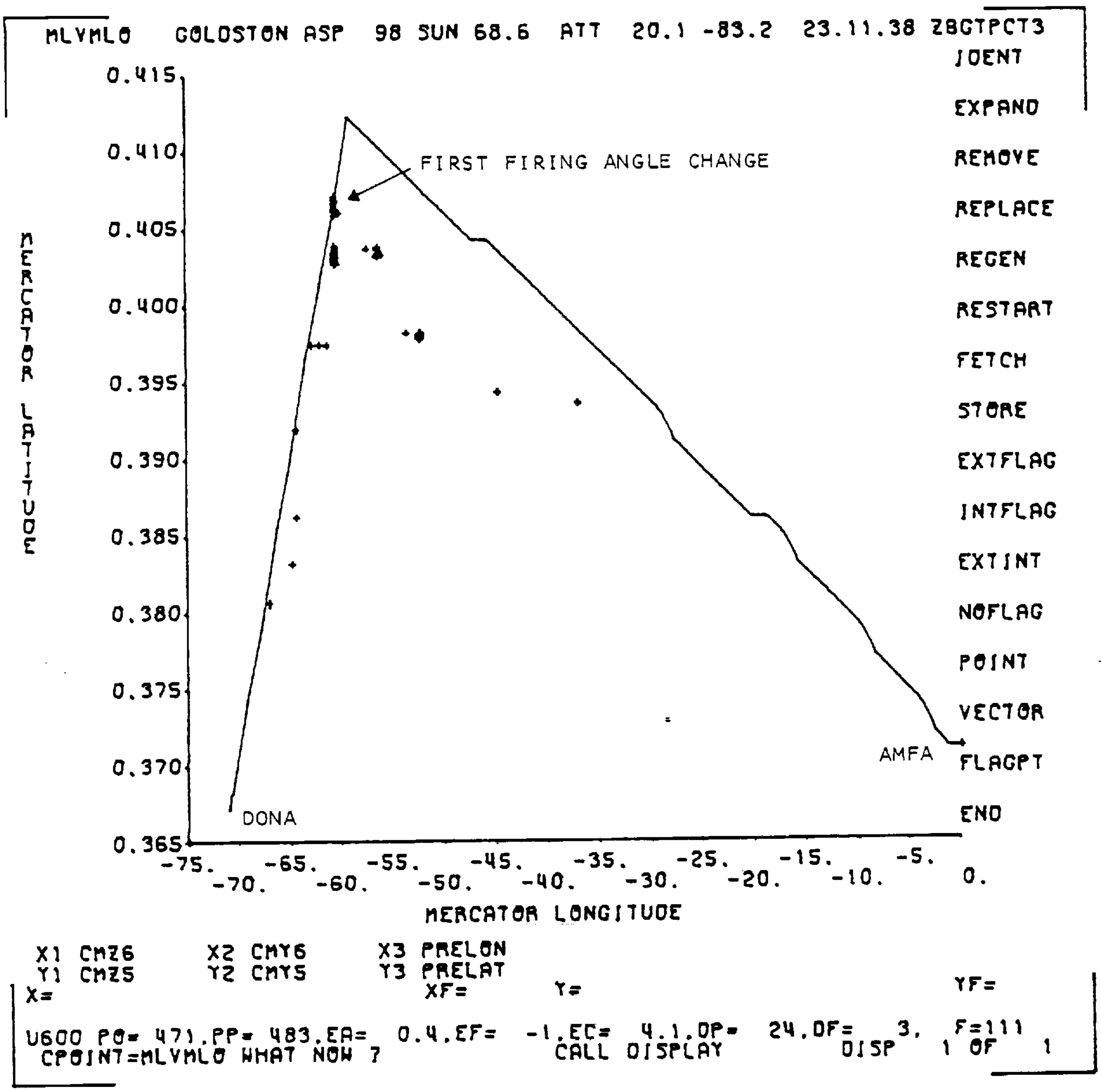


Figure 5-14. Mercator Latitude Versus Mercator Longitude Plot for Predicted Maneuver From AMFA to DONA and Observed Maneuver Prior to Second Firing Angle Change

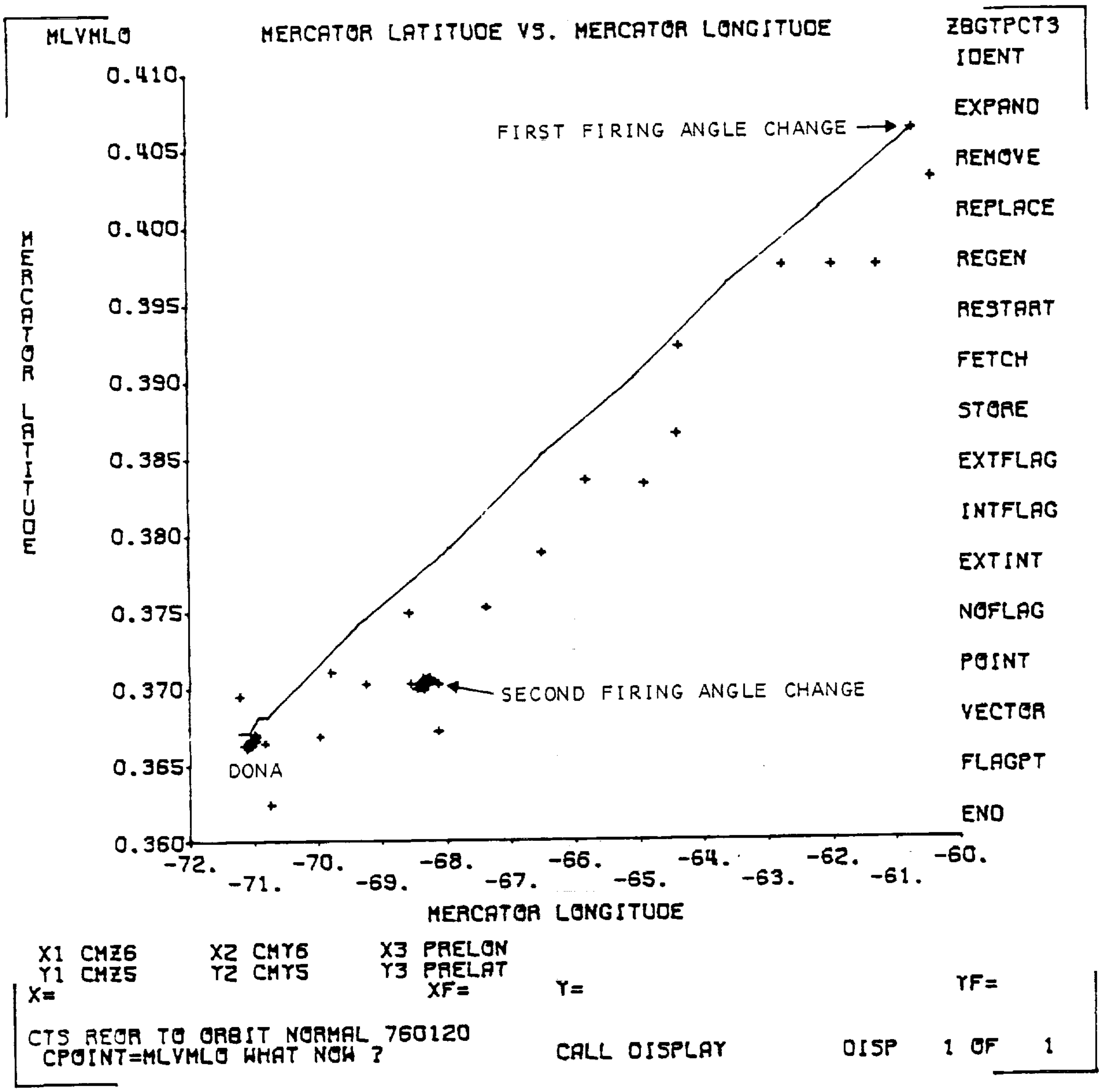


Figure 5-15. Mercator Latitude Versus Mercator Longitude Plot for Maneuver From First Firing Angle Change After AMFA to DONA

Table 5-1. Attitude Control System Command and Performance History

| NO. | ATTITUDE MANEUVER | Ax HTE COMMAND | | PREDICTED RHUMB ANGLE OF MANEUVER (DEGREES) | FINAL PREDICTED ATTITUDE | | FINAL OBSERVED ATTITUDE | |
|---|---|---|---|---|---|---|---|---|
| | | JET START ANGLE (CLOCK COUNTS) | NUMBER OF PULSES | | RIGHT ASCENSION (DEGREES) | DECLI-NATION (DEGREES) | RIGHT ASCENSION (DEGREES) | DECLI-NATION (DEGREES) |
| 1 | INJA TO SVA | 226 | 93 | 108.5 | 198.6 | −10.2 | 198.1 | −11.0 |
| 2 | SVA TO INTA | 218 | 690 | 95.4 | 240.1 | 83.0 | 212.6 | 76.2 |
| 3 | INTA TO FIRST STOP | 203 | 775 | 71.8 | | | 18.6 | 7.7 |
| 4 | FIRST STOP TO SECOND STOP AFTER INTA | 200 | 93 | | | | 18.3 | − 3.1 |
| 5 | SECOND STOP TO THIRD STOP AFTER INTA | 200 | 93 | | | | 17.7 | −14.5 |
| 6 | THIRD STOP TO FOURTH STOP AFTER INTA | 202 | 31 | | | | 17.6 | −18.4 |
| 7 | FOURTH STOP AFTER INTA TO AMFA | 202 | 31 | | 17.4 | −22.9 | 17.3 | −21.9 |
| 8 | TRIM TO AMFA | 212 | 12 | | 17.5 | −23.2 | 17.5 | −23.2 |
| 9 | AMFA TO FIRST FIRING ANGLE CHANGE | 214 | 434 | 87.4 | | | 17.4 | −79.1 |
| 10 | FIRST TO SECOND FIRING ANGLE CHANGE | 224 | 62 | 102.5 | | | 21.7 | −86.5 |
| 11 | SECOND FIRING ANGLE CHANGE TO DONA | 218 | 21 | | 1.8 | −89.2 | 15.8 | −88.8 |

# SECTION 6 - CONCLUSIONS

The major conclusions of the observations and analysis during and after the launch are summarized as follows:

- Spinning attitude sensors performed well. Alignment was good; as a result, only small biases were observed.
- The available perigee data was utilized effectively; as a result, the AMFA was determined to high precision, and extremely close agreement between the desired and observed drift orbit after the apogee motor firing was realized.
- The Ax HTE performed well. Alignment was good; as a result, the observed spin rate variation during attitude maneuvers was very close to the predicted variation.
- Errors in the Ax HTE calibration data were small. The observed rhumb angles of attitude maneuvers were approximately 1.5 degrees larger than predictions, and the observed precession per pulse was approximately 8 percent smaller than that predicted.
- Throughout all the attitude maneuvers, the spacecraft was kept within all the constraints and did not overshoot the target attitude. All attitude maneuvers were completed within 1 degree of the desired attitude.
- The attitude support software performed flawlessly throughout the mission.
- All of the attitude determination and control support requirements were satisfied throughout the National Aeronautics and Space Administration (NASA) phase of the mission.

## REFERENCES


1. Computer Sciences Corporation, CSC/TM-76/6001, Communications Technology Satellite (CTS) Attitude Analysis and Support Plan, G. K. Tandon et al., February 1976

2. Communications Research Centre, SES Leading Edge Output Anomaly, memorandum from A. D. Challoner to D. C. Buchanan, July 31, 1975

3. --, Encoder Bit Rates, memorandum from P. Robinson to W. M. Evans, November 18, 1975

4. --, Encoder Clock Rate - NASA Phase, memorandum from P. Robinson to H. Raine, January 5, 1976